Calibrating New Isotopic and Morphological Tools for Palaeoecological Forest Reconstructions

Thesis submitted in accordance with the requirements of the University of Adelaide for an Honours Degree in Geology

Heather Louise Duff

October 2017

THE UNIVERSITY of ADELAIDE

CALIBRATING NEW ISOTOPIC AND MORPHOLOGICAL TOOLS FOR PALAEOECOLOGICAL FOREST RECONSTRUCTIONS

RUNNING TITLE

Leaf Traits as Indicators of Canopy Closure

ABSTRACT

The ability to identify forest architecture in the geologic past has implications for our understanding of palaeoecological processes. The degree of canopy closure (or density of foliage) effects atmospheric circulation and hydrologic cycling, which in turn, can influence terrestrial temperature and rainfall patterns. Closed canopy forests are characterised by strong gradients in light intensity, which influence the chemistry and morphology of leaves. This study has used isotopic and morphological leaf traits from the modern closed canopy Daintree Rainforest in Queensland, which can also be measured from fossil leaves, to calibrate a multi-proxy tool that characterises the spatial distribution of light intensity. Leaf area index (LAI) was used to quantify forest canopy closure. Changes in carbon isotope ratios ($\delta^{13}C$), leaf mass per area (LMA), undulation index (UI) and cell area (CA) all had linear correlations with increasing LAI from the canopy to the understory. Therefore, these traits can be used as a proxy for reconstructions. However, the magnitude of responses varies between species. A portion of species were unresponsive in UI. Therefore, this proxy may not be suitable for all species. Traits from leaves from beneath a gap in canopy closure and those from a drought experiment, did not deviate from the general gradient seen with LAI. The model used to predict LMA (petiole width^2/ leaf area) did not correspond with measured LMA, and did not characterise the light gradient found within the Daintree rainforest. However, they did predict the average LMA of the rainforest. Investigations into inter-trait variations demonstrate that $\delta^{13}C$, CA and UI correlate with LMA, and CA correlates with UI. Results show several new leaf traits that can be used to identify the degree of shading in closed canopy forests in the fossil record, and demonstrate how light gradients drive variation within a forest.

KEYWORDS

Calibrating, proxy, rainforest, canopy closure, reconstruction, carbon isotope ratio, undulation index.

TABLE OF CONTENTS

LIST OF FIGURES

1. INTRODUCTION

In terrestrial environments, reconstructing forest canopy architecture often relies on the chemistry and morphology of fossilized leaves because they record their immediate environmental conditions during growth (Bush et al., 2017; Coble & Cavaleri, 2015; Dunn et al., 2015; Graham et al., 2014; Farquhar et al., 1989). Leaves are also the most common macrofossil found in fossil assemblages (Bush et al., 2017; Graham et al., 2014). Closed canopy forests, defined by 40% or more biomass coverage (FAO, 1999), are characterised by strong light gradients from the upper canopy to the understory. By analysing leaf traits, it is possible to identify this gradient, and thus infers the degree of canopy closure and ecosystem processes (Graham et al., 2014). Furthermore, canopy closure affects surface albedo, atmospheric circulation and hydrologic cycling, and thus has a substantial control on terrestrial temperature and rainfall distribution (Graham et al., 2014; Boyce et al., 2010; Royer et al., 2007). Therefore, reconstructing canopy closure has significant implications for our understanding of palaeoecological functions and past climates.

Canopy closure is not uniform, rather, it is highly complex. The density of overhanging foliage controls the penetration of light, relative humidity and concentration of CO_2 below and within the canopy (Hollinger, 1989). Therefore, within a single ecosystem, a leaf's physiognomy can correlate with distinct microhabitats, rather than the total forest canopy closure (Dilcher, 1974). While research on quantifying how numerous leaf traits differ within closed canopy forests are beginning to emerge (Dunn et al., 2015; Graham et al., 2014; Kürschner, 1997), few have characterised how the appearance of various

leaf traits can co-vary across many species and microhabitats within a single forest stand (Dunn et al., 2015). To develop reliable proxies that are based on multiple traits, understanding the impact of microenvironments on leaf signatures is imperative.

One of the key chemical traits used to infer canopy closure is carbon isotope ratios. The atmosphere contains two stable isotopes, ^{12}C and ^{13}C (Farquhar et al., 1989). Leaves naturally have a higher concentration of ^{12}C than the atmosphere because it reacts more easily through the photosynthetic pathway (Farquhar et al., 1989; Nier & Gulbransen, 1939). The expression of the ratio in leaves ($^{13}C/^{12}C$) changes in response to photosynthetic rate, atmospheric carbon dioxide composition and available moisture (Bush et al., 2017; Coble & Cavaleri, 2015; Jackson et al., 2012; O'Leary, 1981; Medina & Minchin, 1980), which are ultimately determined by the degree of canopy closure. The "canopy effect" (Graham et al., 2014) describes the characteristic decrease in bulk carbon isotope composition ($\delta^{13}C$) of leaves beneath a closed canopy in a vertical gradient from the upper canopy to the understory (Graham et al., 2014; van der Merwe & Medina, 1991). Higher $\delta^{13}C$ values are found in the upper canopy as increased sunlight drives faster rates of photosynthesis, reducing discrimination against ^{13}C (Coble & Cavaleri, 2015; Graham et al., 2014). In contrast, shaded understory leaves have higher rates of discrimination, and thus have a more negative $\delta^{13}C$ (van der Merwe & Medina, 1989). The strength of this gradient can be used to infer the amount of closure using the diagnostic isotope ranges (Graham et al., 2014).

Canopy closure also affects the atmospheric concentration of carbon dioxide (Graham et al., 2014). On the forest floor, ^{12}C enriched leaves decompose, increasing the ^{12}C

concentration of the atmosphere. This is then taken up by the understory leaves, enriching them with ^{12}C compared to upper canopy leaves (van der Merwe & Medina, 1991; Farquhar et al., 1989). As the accumulation of CO_2 can be disrupted by atmospheric circulation, which is controlled by the amount of canopy closure (Kürschner, 1997), gaps can therefore decrease the gradient depending on their size (Crowley et al., 2012; Farquhar et al., 1989). Environmental stress can further change $\delta^{13}C$. Under drought conditions, leaves close their stomata to reduce water loss which reduces discrimination against ^{13}C (Zhao et al., 2006; Juenger et al., 2005), resulting in less negative $\delta^{13}C$ (Farquhar et al., 1989).

Morphological differences can also be used to indicate whether a leaf grew in sun or shade conditions (Royer et al., 2007). Leaf mass per area (LMA), is a measure of dry leaf mass per unit of light-intercepting leaf area (Cavaleri et al., 2010; Poorter et al., 2009; Markesteijn et al., 2007; Royer et al., 2007; Niinemets et al., 2004; Wright et al., 2004; Ellsworth & Reich, 1992). As plants are sessile organisms, a single tree must be able to maximise the photosynthetic function of leaves with a minimum cost of growth (Markesteijn et al., 2007; Ü. Niinemets, 2001; Jurik, 1986). Therefore, leaves that grow in high sunlight exposure have a thicker blade or denser tissue because they become more concentrated in smaller, denser cells packed with photosynthetic components (Coble & Cavaleri, 2015; Poorter et al., 2009; Wright et al., 2004). In contrast, shaded leaves increase leaf blade area to improve light capture where light availability is reduced (Coble & Cavaleri, 2015; Poorter et al., 2009). Previous studies conducted on contemporary forests consistently show that leaves in the understory display a lower LMA compared to those in the high light canopy (Coble & Cavaleri, 2015; Oguchi et

al., 2005; Turney et al., 2002; Kürschner, 1997; Oberbauer & Strain, 1986). However, LMA is often not studied in ancient ecosystems as it cannot be directly measured from leaf fossils (Royer et al., 2007). As it is such a useful measure of ecological adaptation, models have been developed that can calculate leaf mass from the petiole width normalised for leaf area, which are two variables commonly measurable from the fossil record (Royer et al., 2007; Givnish & Vermeij, 1976). Petiole width is useful because in general, heavier leaves require more substantial petioles for support (Royer et al., 2007).

Micromorphological features of leaves, such as the amount of undulation (or curvature) of anticlinal cell walls in the epidermis, and the area of those cells (CA), can differentiate between leaves grown in high or low light (Bush et al., 2017; Jacques et al., 2011; Xiao et al., 2011; Wagner-Cremer et al., 2010; Kürschner, 1997; Kerp, 1990; Watson, 1942). Cell wall undulation is a comparative measure of the perimeter of the cell compared to the perimeter of a circle with the same area, where the ratio is defined as undulation index (UI) (Kürschner, 1997). Leaves exposed to direct sunlight have a higher epidermal cell density due to rapid cuticle hardening (Watson, 1942). Comparatively, leaves growing in low light conditions experience slower hardening of cell walls and increased cell expansion (Kürschner, 1997; Watson, 1942). Therefore, the cell walls can become more undulated and have increased CA compared to leaves exposed to direct sunlight (Kürschner, 1997). The UI response to light exposure also differs among species (Bush et al., 2017). Therefore, variation in UI not only exists between the upper and the lower canopy, but potentially between species.

In tropical rainforests, mosaics of canopy closure are driven by the complex interaction of topography, damage incurred by frequent tropical storms (Bellingham, 1991; Denslow, 1980), and complex vegetation responses that result in gaps created by treefalls (Grove et al., 2000). As the degree of closure regulates atmospheric circulation and light penetration, it affects the way that leaf traits are expressed in varying levels of the rainforest. For example, leaves in the understory beneath a gap experience different environmental conditions than understory species beneath a closed canopy (Jackson et al., 2012). Furthermore, LMA, UI and CA can differentiate between leaves exposed to sun or shade, but they cannot infer the placement of growth in the canopy. For reconstructions which are reliant on proxies to reconstruct these environmental gradients, this can complicate results because leaves in the understory no longer display traits consistent with leaves beneath a closed canopy (Jordan et al., 2014). Consequently, a comprehensive understanding of the sources of trait variability in an ecosystem is imperative for accurate reconstructions.

An effective method of quantifying how these traits differ within a rainforest, is to quantify the canopy closure in terms of leaf area index (LAI). LAI is calculated by comparing the amount of foliage blocking the sky from beneath the canopy at a given point (Jupp et al., 2009), defined as m^2 of leaf area per m^2 of ground area. LAI can vary from fully exposed (0) to a closed canopy (>7) (Figure 1). UI has been used as a method for estimating LAI from fossilized phytoliths which preserve the cell shape, and thus can be used to infer the amount of canopy closure (Dunn et al., 2015). This comparisons

was calibrated by using LAI measurements from extant forests to compare with those from fossil records (Dunn et al., 2015).

Figure 1: Hemispherical photos of varying canopy closure from understory sample sites in The Daintree Rainforest (2017). LAI measurements were taken adjacent to sampling points with a Licor LAI-2200. (a) The understory-gap site, with an approximate LAI of 3.36. (b) The understory control site (closed canopy), with an approximate LAI of 6.18.

Linking multiple leaf traits that correlate with LAI or other informative leaf traits can enable more accurate and descriptive within canopy reconstructions (Bush et al., 2017; Dunn et al., 2015; Royer et al., 2007; M. J. Lockheart et al., 1998b). However, studies within extant forests rarely incorporate leaf traits beyond two measurement types. In addition to the method to calculate LMA from petiole width (Royer et al., 2007), $\delta^{13}C$ values have been used with UI to evaluate whether variable light within a closed canopy forest is driving changes in leaf traits (Bush et al., 2017). The comparison of stomatal index and $\delta^{13}C$ has revealed correlating features that indicate whether leaves grew in sun or shade conditions (M. Lockheart et al., 1998a). If multiple correlating leaf traits are able to be characterised it could provide the basis for the creation of a significant

proxy used for reconstructing canopy closure.

This study investigates LMA, UI, CA and $\delta^{13}C$ values of leaves in the sun-exposed upper canopy and shaded understory of the Daintree Rainforest, Northern Queensland. An additional comparison is made using a subset of species from varying levels in the rainforest with LAI measurements. A comparison of canopy samples from a control and drought site within the canopy, and a comparison of understory samples from beneath a closed canopy and a gap will also be included. In characterising the natural variation of these traits within a closed canopy rainforest, the aim is to provide a better understanding of the role that microenvironments and canopy closure has in determining leaf traits.

It is hypothesised that measurements of UI, LMA, $\delta^{13}C$ and CA will display variations between the upper canopy and understory. To test whether differences are correlated with canopy closure and not alternate factors, traits will be compared along a gradient of leaf area index (LAI). With this, it is hypothesised that $\delta^{13}C$ of leaves will become more negative from the canopy to the understory, similar to relationships seen in previous studies (Graham et al., 2014). Samples from the drought site will have a less negative $\delta^{13}C$ than those in the control site of the same LAI. The magnitude of UI responses will differ among species (Bush et al., 2017); species which do have a response, will decrease in UI with increasing exposure (decreasing LAI); species from within the drought site will have a lower UI than the control sample; cells grown under high light will have a smaller CA compared to those in shaded conditions, and samples from within the drought site will have a smaller cell size compared to control samples.

Furthermore, it is hypothesised that leaves in the upper canopy will have a higher LMA than those in the understory. Leaves from the understory gap (US-G) site will not have the same trait as those beneath the closed canopy understory site (US-C). The model developed by Royer *et al*. (2007) enables the reconstruction of LMA from petiole width and leaf area. It is hypothesised that the same model is applied to this data set, the model will enable an accurate prediction of the measured LMA. Finally, leaf traits which have significant correlations with LAI will co-vary with other traits measured from the same leaf.

2. SITE BACKGROUND

The Daintree rainforest is part of the wet tropical region of north-eastern Queensland. Globally, this region hosts the oldest continuous rainforest whose ancestors can be traced back to the forests of the Late Cretaceous (Costion et al., 2015; Christophel & Greenwood, 1989). Though its current distribution is restricted to less than 0.1% of the continent, a fossil record rich in macro and micro specimens suggests that rainforests were once wide spread across the continent (Jordan et al., 2014; Dettmann, 1994). Changes in rainforest distribution were driven by a variety of geological processes, including major global positioning shifts and a fluctuating climate (VanDerWal et al., 2009). While the climate was cooler and more temperate, the rainforests were widespread until the continent finally detached from Antarctica *c.* 38mya (Costion et al., 2015). As the climate cooled and aridified, the rainforests were forced to retreat towards the eastern coast into elevated plateaus that were created during the Tertiary. These climactic pockets enabled the survival of many species of flora (Greenwood & C Christophel, 2005), ultimately leading to the uniquely diverse ecosystem which exists today (Costion et al., 2015).

Now considered 'relicts' of the ancient Gondwanan forests, many of the present species in the Daintree Rainforest provide evidence of the evolution of angiosperms through their lineages (Hill, 2004; Christophel & Greenwood, 1989; RSCQ, 1986). Due to many extant species being similar to those found in the fossil record, they are ideal for calibrating proxies for climate, vegetation and palaeoreconstructions, which rely on leaf physiognomy.

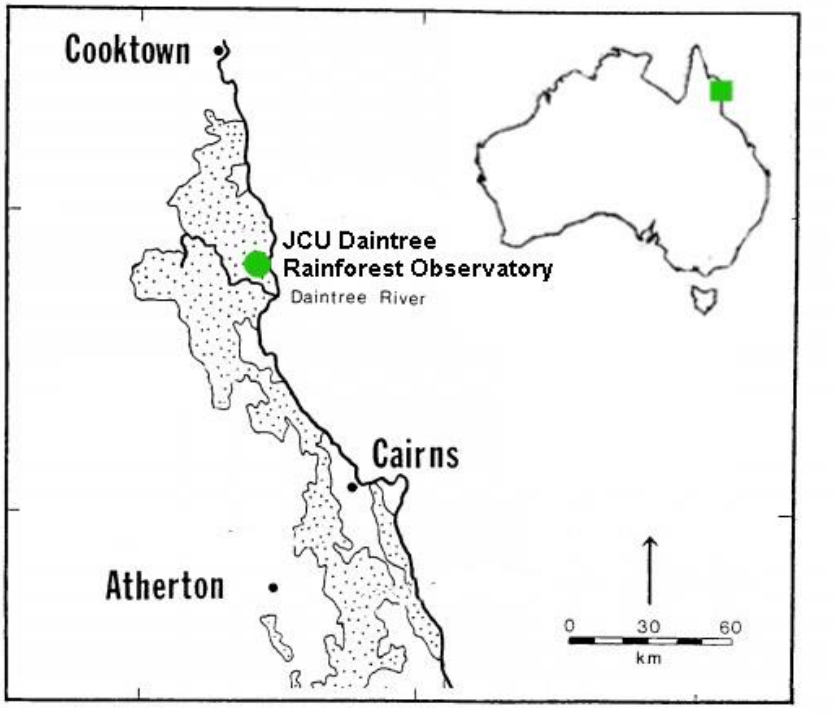

Figure 2: The location of the James Cook University Observatory on the east coast of northern Queensland. The green box indicates the approximate region illustrated. Stippled areas indicate the Wet Tropics World Heritage Area of north Queensland. Images adapted from Trenerry et al., (1994) and Dragovich and Grose (1990).

3. METHODS

3.1 Upper canopy and understory samples

Leaf samples were obtained from the James Cook University Daintree Rainforest Observatory, situated on the low-land coastal plains of the Daintree rainforest. Samples of 15 species were taken for analysis to The University of Adelaide from the understory and upper canopy, along with LAI measurements. For species comparison between rainforest levels, fully sun-lit upper crown samples and associated $\delta^{13}C$, LMA, leaf area and petiole measurements were supplied by Dr Alex Cheesman, James Cook University, College of Science and Engineering (centre for Tropical Environmental and Sustainability Studies). Understory samples were supplied by Dr Lucas Cernusak, James Cook University, College of Science and Engineering (centre for Tropical Environmental and Sustainability Studies) and analysed at the University of Adelaide.

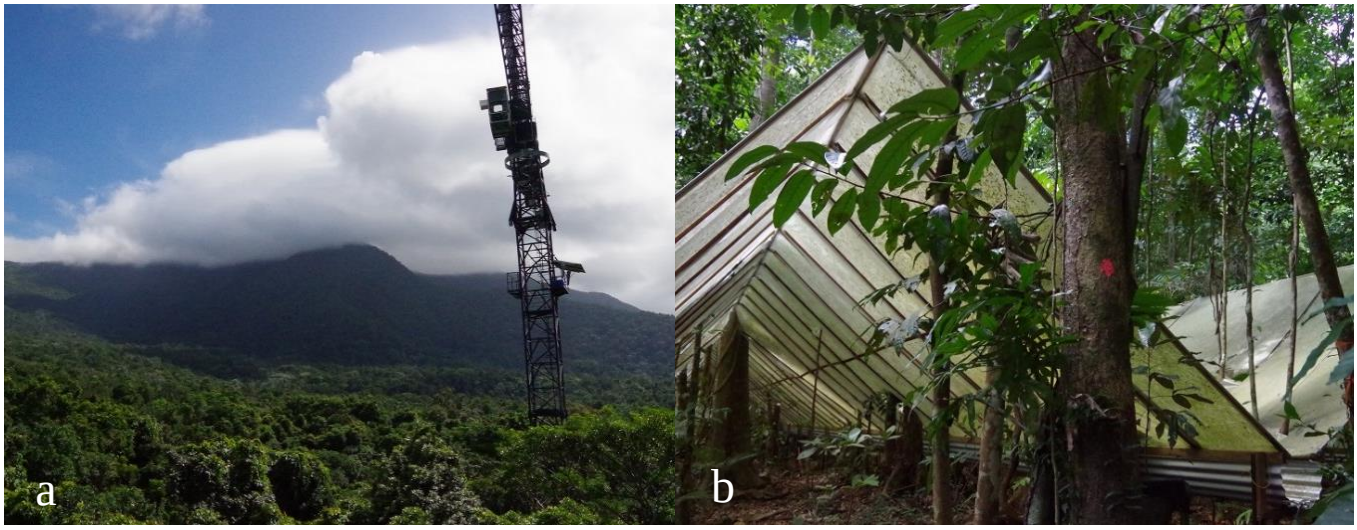

Figure 3: Sampling sites from the James Cook University Daintree Rainforest Observatory. The canopy crane allows access to the upper crown and interior canopy regions of the control and drought sites (a). Plastic sheets over the base of the drought site to prevent rainfall reaching roots of trees (b).

3.2 LAI comparison samples

Leaves from five species (*Argyrodendron peralatum, Myristica globosa ssp. muelleri, Endiandra microneura, Cleistanthus myrianthus* and *Rockinghamia angustifolia*) were selected because of their prevalence in all heights and areas of the study site. The leaves were taken from three levels to capture the variability in LAI. These levels were the upper crown (UC, fully exposed), interior crown (IC, partial cover by surrounding vegetation but not overhanging foliage) and the understory (US, closed canopy, 40% or more cover by foliage (FAO, 1999)). In addition to the samples from the closed canopy understory site (US-C), samples were also taken from beneath a significant canopy gap (Gap understory, US-G). Leaves were also sampled from UC and IC levels within the drought experiment site for comparison with the UC and IC of the control site.

3.3 Sampling procedure

A total of ten locations were used for canopy sampling, made accessible by the Daintree Rainforest Observatory's canopy crane (Figure 2a). Each upper canopy sample consisted of six leaves taken from a single branch with similar exposure and minimal insect damage. For the canopy samples with six leaves, a range of leaf sizes (small, medium and large) were chosen to avoid bias. Three were then dried for LMA, and three were used for UI analysis. Samples referred to in this analysis are comprised of three leaves from the same branch. Additional canopy samples were taken from five trees in the UC and IC in the drought experiment (Figure 2b) (Laurance, 2015), run by Associate Professor Susan Laurance, James Cook University, College of Science and Engineering. Two canopy samples were taken from each location (UC and IC). At least one sample of each species were taken from US-C and US-G sites accessible by foot. Understory samples consisted of only three leaves because many trees were juvenile and

had sparse foliage. Leaf samples were frozen before being transported for analysis to The University of Adelaide and remained frozen until required for analysis. Epidermal tissue for UI and CA was removed from fresh leaves. Leaves were oven-dried before measuring LMA and $\delta^{13}C$.

3.4 Leaf area index (LAI)

Canopy closure was quantified with an LAI-2200 Plant Canopy Analyser (Li-COR Inc., 2010 , loaned by Christina Macdonald, Terrestrial Ecosystem Research Network, The University of Adelaide. LAI was estimated by comparing a fully exposed above canopy reading (A reading) with one measurement taken adjacent to each sample point (B reading). For understory samples, A readings were taken in a clear, open field adjacent to the rainforest prior to any B readings.

3.5 LAI data processing

Recorded LAI data was processed with the FV2200 program by comparing the closest A reading in time with each B reading. The LAI-2200 quantifies canopy closure using 5 zenith rings, measuring foliage blocking the sky from the sampling point in a hemispherical view. A readings, being fully exposed, should have a lower LAI than any B reading. However, some A measurements were lower than the B reading in the outermost ring. This difference is attributed to interference from the surrounding mountains or the crane boom. To correct LAI, the outermost ring (5^{th}) was removed from comparison as advised by the LAI-2200 manual.

3.6 UI and CA

Each sample comprised measurements from three leaves. 38.48mm^2 sections were cut from each leaf and the fresh leaf epidermis was cleared of mesophyll tissue using chromic acid. The epidermal tissue was then dyed and mounted onto slides in glycerin jelly. An Olympus AX70 microscope was used to take three photographs per sample of the abaxial epidermis under 40x magnification. For each photograph, five well-preserved cells were traced using a stylus in ImageJ, which measured the cell perimeter and area. In slides where there was little epidermis intact, multiple images were taken until 15 cells per leaf were able to be traced. Each sample is therefore comprised of an average of 45 cells. The measure of undulation was calculated by the following equation (Kürschner, 1997):

$$UI = \frac{C_e}{C_0} = \frac{C_e}{2 \times \pi x \sqrt{\frac{A_e}{\pi}}} \quad (1)$$

Where C_e (µm) is the circumference of the cell, C_0 is the circumference of a circle with the same area as the cell and A_e (µm^2) is the area of the cell (Kürschner, 1997). To determine the measurement error in UI, a single cell was traced 15 times. For a cell with an average UI of 1.05, the range in UI was 0.038. As this range was small, subsiquent analysis were performed by tracing each cell once.

3.7 LMA and petiole width

Leaves were scanned using a scanner and traced using ImageJ to calculate the area and perimeter. Dried leaves were then weighed on a Sartorius R200D Electronic Semi-

Microbalance and measured in grams. LMA was then calculated by the following (Royer et al., 2007):

$$LMA = M/A \quad (2)$$

Where M is mass (g) and A is area (m^2). Petiole width was measured with a micrometre. A scaling relationship between leaf area and petiole width was then used to predict LMA, in accordance with the following equation:

$$predicted\ LMA = (Petiole\ Width)^2/(Leaf\ Area) \quad (3)$$

With petiole width in m, and leaf area in m^2 (Royer et al., 2007). 131 additional measurements from US and UC samples provided by Dr. Alex Cheesman were included in this analysis. Samples for this analysis were not averaged by branch, rather a single leaf's petiole width and leaf area was used to compare predicted LMA against measured LMA.

3.8 Carbon isotope analysis

Leaf samples were analysed for $\delta^{13}C$ with a EuroVector EuroEA elemental analyser, in line with a Nu Horizon CF-IRMS by Mark Rollog at The University of Adelaide. Samples were homogenised by grinding three leaves with a Retsch MM 400 Mixer Mill into one sample, and a single $\delta^{13}C$ value was produced for each sample.

3.9 Statistical analysis

All analyses were done using the program GraphPad. Each trait ($\delta^{13}C$, LMA, Cell area and UI value) was first compared within species between the US and UC. To display variance between the traits taken from the drought UC and control UC, an unpaired t-test was performed for each leaf trait. The parametric test assumed a gaussian distribution. A significance level of $P<0.05$ was considered for this comparison. As no significant results were found at $P<0.05$, all drought and gap sample data was included in the subsequent analysis. Gap samples were compared by species between the US-C and US-G. Leaf traits were compared against LAI with a least-squares egression, to ob obtain relevant statistical values (regression equation, r^2 and P-values). Measurements from all three data sets were used to scale LMA against petiole width, to test the method of reconstruction calculated by Royer et al. (2007). Traits were then tested for co-variance with least-squares regression. As Cell area and LMA had a non-linear response, a $\log_{10}$ transformation of LMA and cell area was applied to the data to obtain a linear equation.

4. OBSERVATIONS AND RESULTS

4.1 Characterisation of understory and canopy crown species traits

Species displayed variable responses of traits between canopy levels (Figure 4). There was a consistent change of $\delta^{13}C$ and LMA in all 15 species between the US and UC, although each response varied in magnitude (Figure 4a & 4b). $\delta^{13}C$ had less negative values in the canopy crown and more negative values in the understory (Figure 4a). For

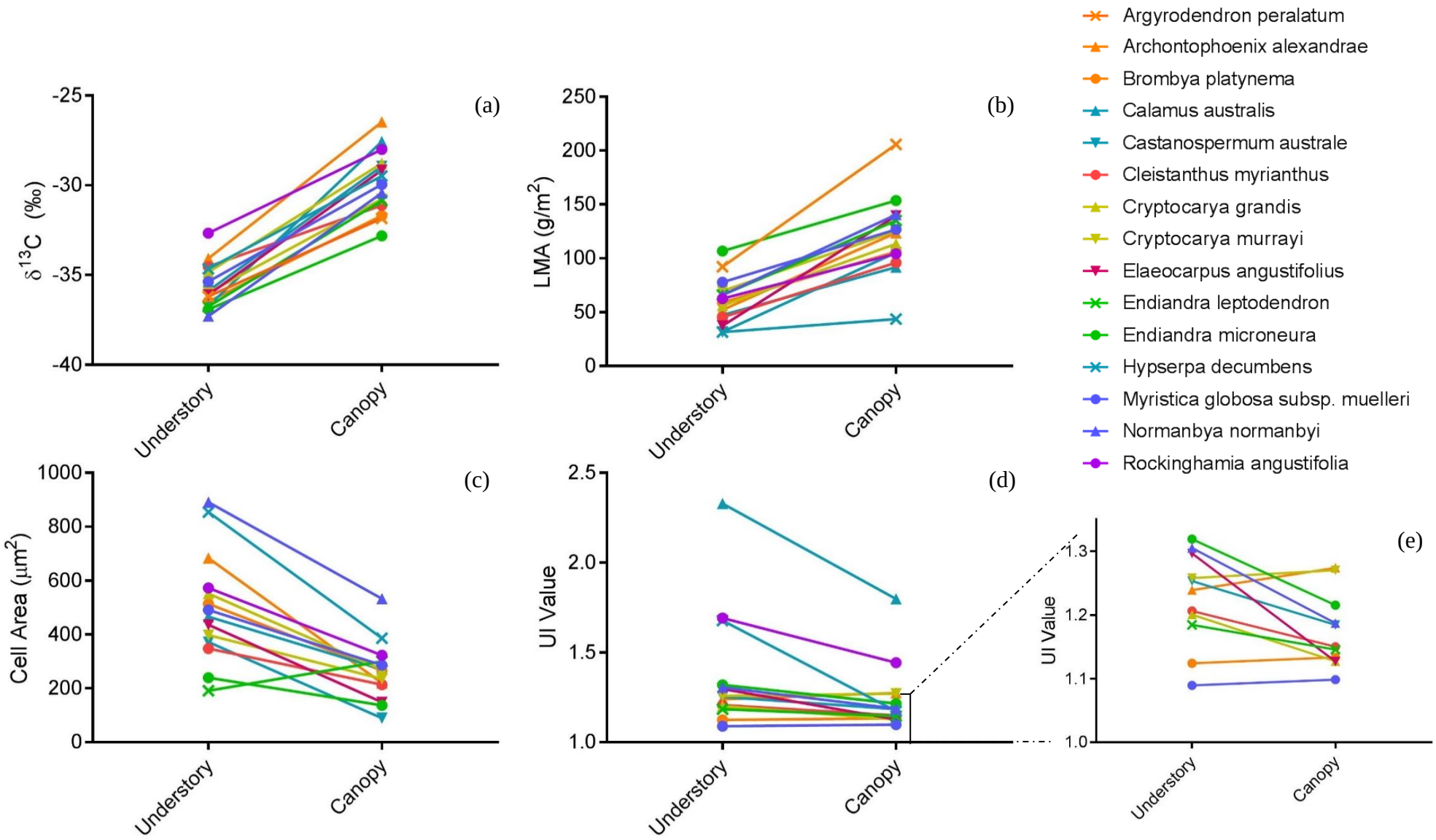

Figure 4: Leaf trait comparison between UC and US samples. (a) $\delta^{13}C$ values. Values are presented in per mil (‰). (b) Leaf mass per area (LMA) of US and UC samples. (c) Cell area of US and UC samples. (d) Undulation index (UI) of US and UC samples. (e) An expansion of UI ranges found in in Figure 3d (approximate UI range: 1.0 to 1.4) for clarity. Responses of *Calamus australis*, *Rockinghamia angustifolia* and *Hypserpa decumbens,* have been removed in Figure 3e.

LMA, all 15 species displayed a response of a higher LMA in the canopy crown (Figure 4b). CA also changed with forest position, showing a decrease in cell size from US to UC (Figure 4c) with one exception. *Endiandra leptodendron* showed an increase in cell size from US to UC. *Calamus australis* and *Hypserpa decumbens* displayed the largest response between US and UC. *Myristica globosa*, *Brombya platynema*, *Archontophoenix alexandrae* and *Cryptocarya murrayi* displayed either little or no response.

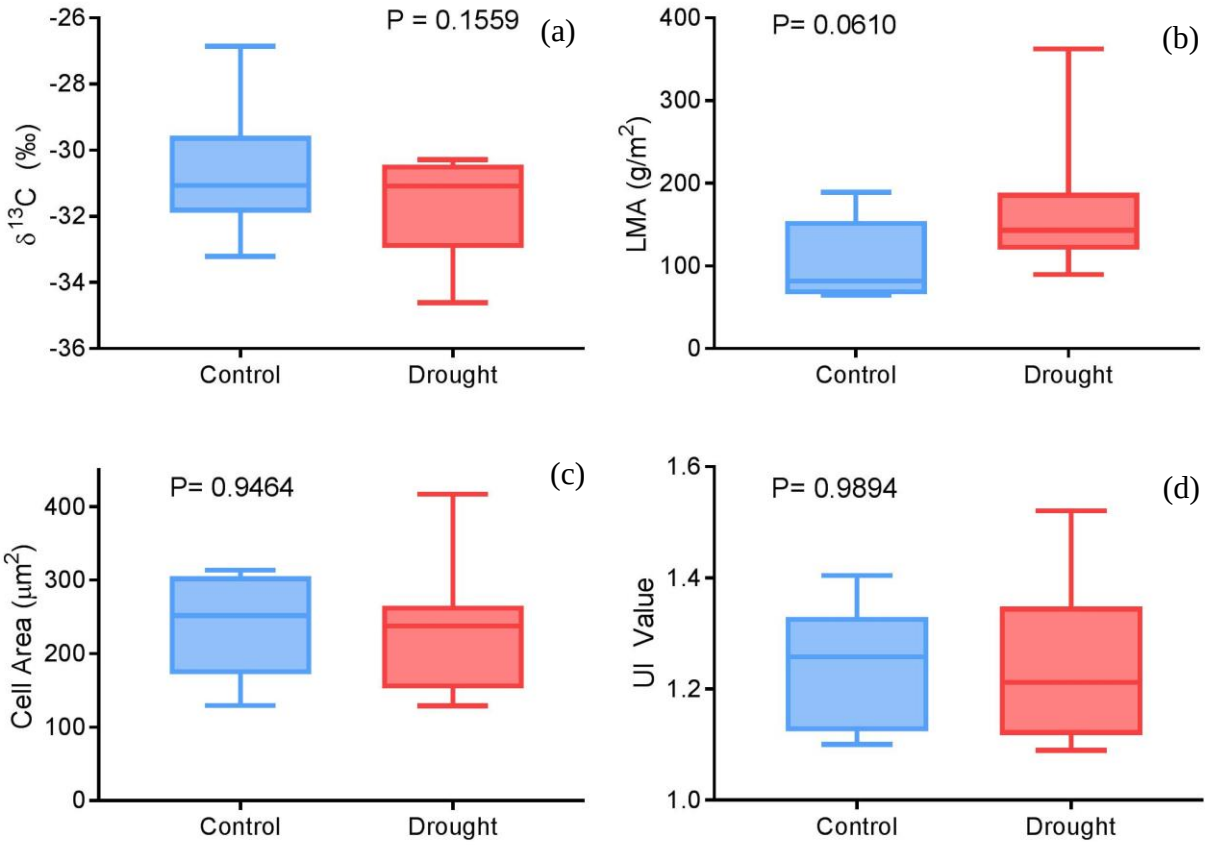

Figure 5: Comparison of mean values of samples taken from UC and IC leaf samples, from the control and drought sites. (a) $\delta^{13}C$ values of samples (b) leaf mass per area (LMA) (c) Cell area (CA) (d) Undulation index value (UI). Box plots characterise the distribution, with the upper and lower limit of the box indicating 25th and 75th percentile. The horizontal line within in the box indicates the median value. Associated r^2 for each comparison (unpaired t-test) are displayed.

4.2 Influences of drought treatments in the canopy and gaps in canopy closure on the understory

There was no difference in $\delta^{13}C$, LMA, CA or UI of leaf traits taken from the control site drought sites (Figure 5). Species had variable responses between the control and gap sites (Figure 6). *M. globosa* and *R. angustifolia* displayed a decrease in $\delta^{13}C$, while. *E. microneura* had a large increase. Both *C.myrianthus* and *A. peralatum* had no alteration between sites. LMA responses to the canopy gap were also variable (Figure 5b). A general increase in LMA was seen beneath US-G of all species except *M.globosa*, which had a distinct decrease. CA decreased from the US-C to US-G, the only species with an increase was *E. microneura.* UI was non-responsive in all species except for *R. angustifolia*, where a distinct decrease occurred.

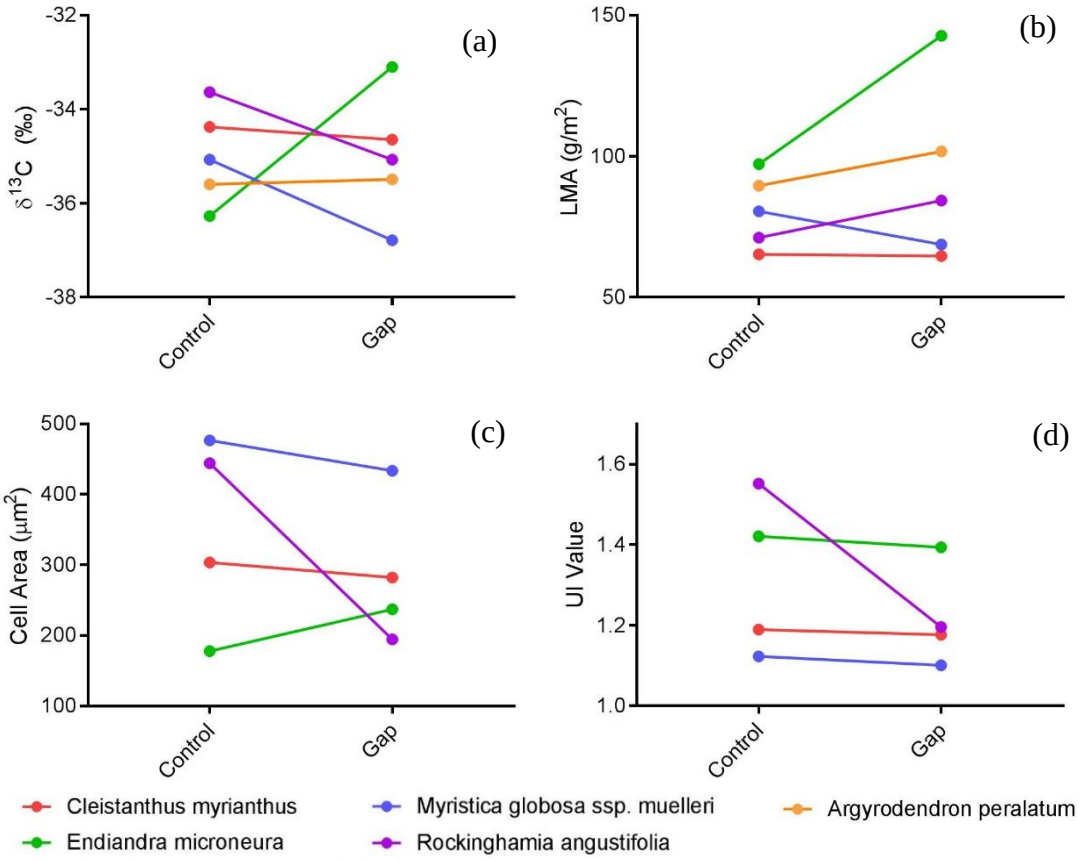

Figure 6: Mean values of leaf samples from the US-G and US-C sample sites. Samples are presented as species averages for each site. (a) $\delta^{13}C$ values of samples (b) leaf mass per area (LMA) (c) Cell area (CA) (d) Undulation index value (UI).

4.3 Comparing species trait responses to leaf area index (LAI)

Figure 7 compares each trait response by species to LAI. The $\delta^{13}C$ of all species increased with decreasing LAI, becoming more ^{13}C enriched towards the high-exposed canopy levels, with a less negative $\delta^{13}C$ (Figure 7a). The most significant responses were seen in *A. peralatum* (P=0.0023) and *M. globosa* (P=0.0020), which also had a strong fit ($r^2 = 0.93$ and $r^2 = 0.87$, respectively) (Table 1). At a 0.10 significance level, *C. myrianthus* (P=0.096, $r^2 = 0.45$) and *E. microneura* (P=0.099, $r^2 = 0.53$) also displayed significant trend, although they did not have a good fit. *R. angustifolia* was the only species which displayed a lack of significance with a p-value of 0.174.

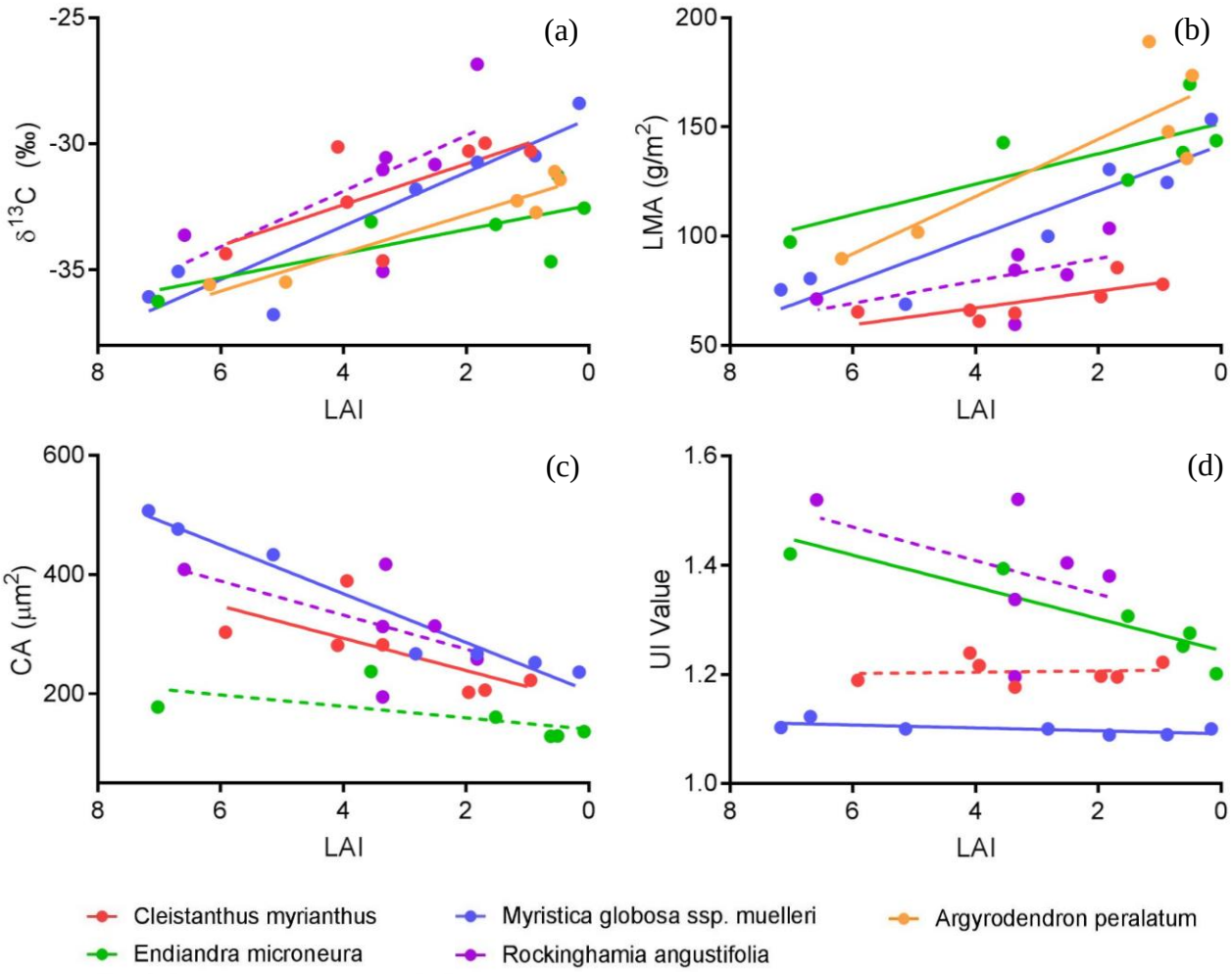

Figure 7: Leaf trait responses to measured LAI by species. (a) $\delta^{13}C$ (per mil, ‰) (b) leaf mass per area (LMA) (c) Cell area (CA) (d) undulation index (UI). Solid lines indicate statistically significant linear regressions at a 0.10 level, dashed lines indicate non-significant responses. LAI ranges from 8 (most shaded) to 0 (fully exposed). Statistical values are in Table 1. The associated standard deviations can be found in Appendix C.

		A.peralatum	*C. myrianthus*	*E. microneura*	*M. globosa ssp. muelleri*	*R. angustifolia*
$\delta^{13}C$ (‰)	r^2	0.93	0.45	0.53	0.87	0.41
	P-value	0.002***	0.096*	0.099**	0.002***	0.174 (NS)
LMA (g m^2)	r^2	0.71	0.57	0.61	0.84	0.30
	P-value	0.033**	0.048**	0.067*	0.003***	0.260 (NS)
CA (µm)	r^2	NA	0.48	0.38	0.95	0.30
	P-value	NA	0.0807*	0.1958 (NS)	0.0002 ***	0.263 (NS)
UI Value	r^2	NA	0.01	0.84	0.45	0.17
	P-value	NA	0.839 (NS)	0.009*	0.097 *	0.417 (NS)

Table 1: Statistical results for the linear regression of species traits with to LAI (Figure 6). For each measured trait, the r^2 and P-value is presented. *A. peralatum* is exempt from UI and CA because clearing methods were not successful. Statistical significance levels are indicated by the following: * = 0.01, **0.05, *0.10. NS = non-significant.**

Only three species (*A. peralatum* (P = 0.0331), *C. myrianthus* (P=0.0769) and *M. globosa* (P=0.0036) displayed a significant positive correlation in LMA with decreasing LAI (Figure 7b). *A. peralatum* and *M. globosa* have a moderately good fit. The two species which were unresponsive to LAI changes were *R. angustifolia* (P=0.2602) and *E. microneura* (P=0.6771) (Table 1).

CA demonstrated a significant negative correlation with decreasing LAI in two species, *C. myrianthus* (P=0.0807) and *M. globosa* (P=0.0002) (Figure 7c). Although the trends of *E. microneura* and *R. angustifolia* displayed the same negative correlation, these results were non-significant (P= 0.1958 and 0.2331, respectively). *M. globosa* was the only species with a good fit (r^2 = 0.95).

Species showed variable UI responses to LAI (Figure 7d). A significant correlation was shown for *M. globosa* (P= 0.0970) and *E. microneura* (P=0.0099) (Table 1). *E. microneura* was the only species with a good fit (r^2 = 0.84). No significant correlation

was seen in *C. myrianthus* (P=0.8393) or *R. angustifolia* (P=0.3320). *A.peralatum* was not analysed for UI or CA because clearing methods were unsuccesful.

When carbon isotope values of all species were compared against LAI, a significant positive linear correlation was observed (P=<0.0001) (Figure 8).

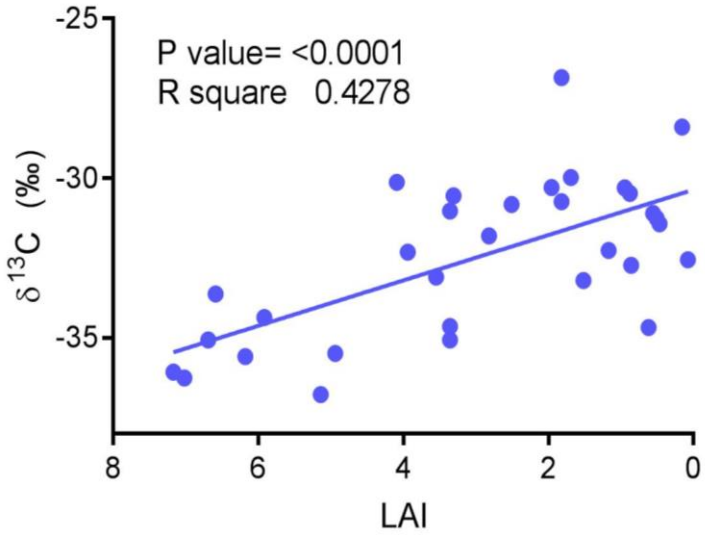

Figure 8: Linear regression of $\delta^{13}C$ values from all species with variable LAI. Assocaited r^2 and P-value are displayed. LAI is displayed from highest number (8) to lowest (0) and indicates from left to right, a higher percentage of cover towards full exposure. Values are means of three leaves per sample.

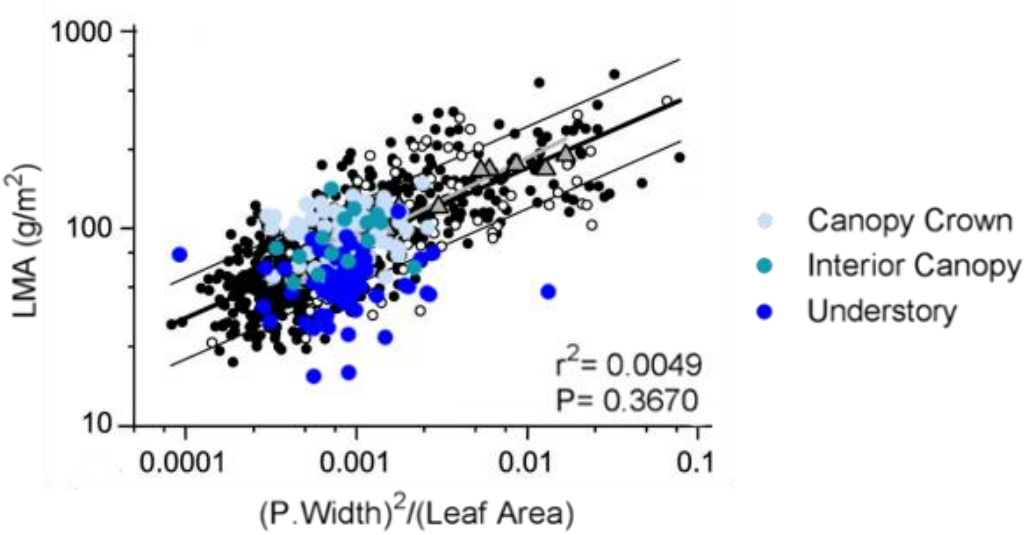

Figure 9: The scaling of petiole width (m^2) and leaf area (m^2) with measured LMA (g/m^2) (blue data points) overlain on modelled data from Royer et al., (2007) (black data points). Solid trend lines indicate linear regression of data, thin lines are ±95% prediction intervals (Royer et al., 2007; Sokal & Rohlf, 1981). The associated r^2 and p-value is from a linear regression of blue data points.

A non-linear response was seen when predicted LMA was compared to measured LMA (Figure 9). The distribution of data lied within the 95% confidence intervals.

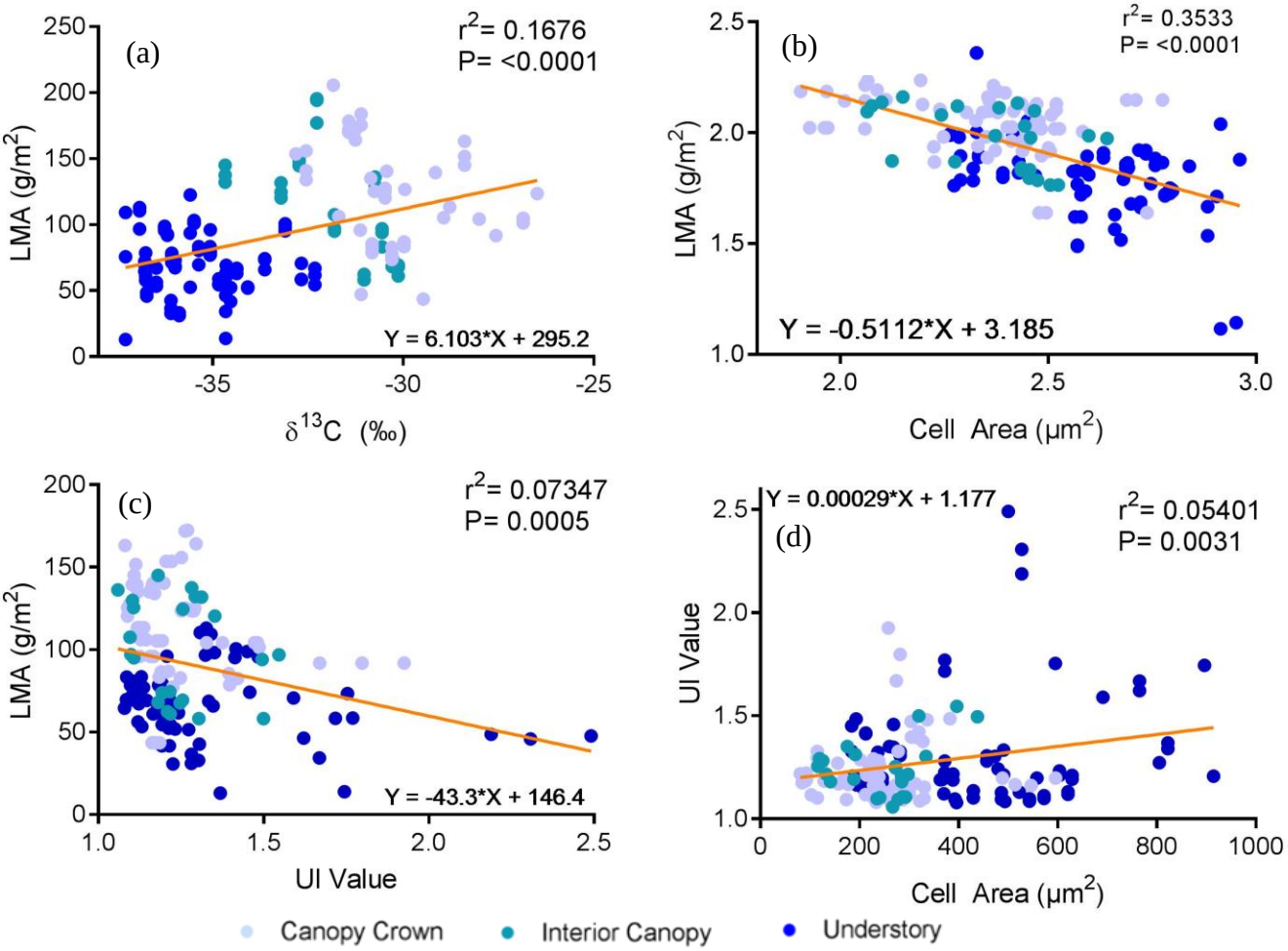

Figure 10: Significantly correlated leaf trait comparisons. The associated r^2, P-values and regression equations from each analysis are presented from the linear regression. (a) $\delta^{13}C$ with leaf mass per area (LMA) (b) Log_{10} transformed data of CA and LMA. Associated r^2 and P-value is calculated from the transformed data. (c) LMA and undulation index (UI) (d) CA and UI. Non-significant results can be found in Appendix B.

Three leaf traits displayed weak, but significant, correlations with LMA (Figure 10). $\delta^{13}C$ displayed a significant positive linear correlation (P=<0.0001) with LMA (Figure 10a), and UI displayed a significant negative linear correlation (P=0.0005) (Figure 10c). CA displayed a non-linear response, and thus was log-transformed (Figure 10b). The

linear regression of log transformed CA was significantly corelated with log-transformed LMA (P=<0.0001). CA also had a positive linear relationship with UI (P=0.0031) (Figure 10d).

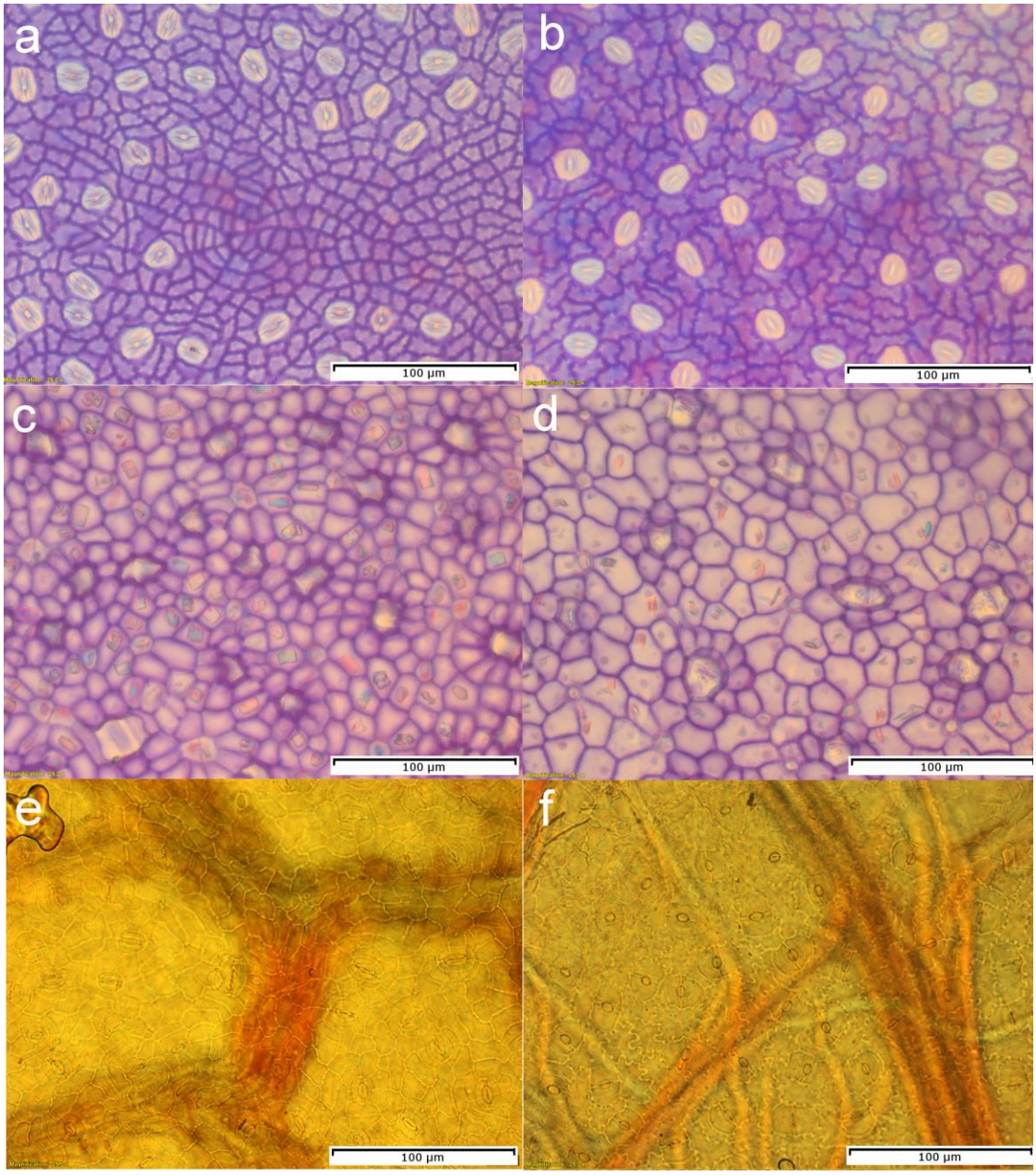

Figure 11: Cleared lower epidermal tissue displaying the undulation of cell walls from different light environments. (a) *Endiandra microneura* UC sample, average IU is 1.27 (b) *Endiandra microneura* US-C, average UI of 1.39. (c) *Myristica globosa ssp. muelleri* canopy control, average UI of 1.11. (d): *Myristica globosa ssp. muelleri* US-G, average UI of 1.12. (e) *Rockinghamia angustifolia* US-G sample, averate UI of 1.20 (f): *Rockinghamia angustifolia* drought IC sample, average UI of 1.49. Samples a to d dare dyed with crystal violet. Samples e to f are stained by chromic acid. Cuticles are under 25.5x magnification. Scale is 100µm.

5. DISCUSSION

5.1 Differences between understory and upper canopy leaf traits

To test whether trends seen in previous studies are apparent in the Daintree Rainforest, a comparison of samples from US and UC was performed. The results showed higher LMA in the upper canopy and lower in the understory (Figure 4b), consistent with findings from previous research (Graham et al., 2014; Cavaleri et al., 2010; Poorter et al., 2009; Markesteijn et al., 2007; Royer et al., 2007; D. S. Ellsworth & Reich, 1993; Jurik, 1986). Canopy placement corresponded to $\delta^{13}C$ values, consistent with relationships found in other forest canopies (Figure 4a) (Coble & Cavaleri, 2015; Graham et al., 2014; Jackson et al., 2012; Garten & Taylor, 1992). However, micromorphological features did not show the same response for each species. UI is not only variable among species in the magnitude of change between sites, but some species display no response at all (Figure 4d). *C. australis* displayed higher UI and a strong negative correlation with canopy level (Figure 4d). *M. globosa* in contrast, has no response to canopy level and thus could not be used for UI analysis on fossils. This supports that UI is species specific (Bush et al., 2017). Nonetheless, for unresponsive species, forest dynamics could be reconstructed from alternate leaf trait analysis. A common problem for palaeoecologic interpretations is that only part of the vegetation is preserved (Kerp, 1990). An incomplete leaf fossil from *M. globosa* for example, though having no response in UI, could be measured for CA (Figure 4c). For CA, all species except *E. leptodendron*, displayed the same decreasing trend from the understory to the canopy. *E. leptodendron* also had no change in UI. Therefore, it is necessary to accurately identify species that are suitable for certain trait analyses. In summary, $\delta^{13}C$

and LMA display a consistent response to LAI, but UI and CA display variable responses among species.

While the differences in foliar chemistry and morphology have displayed promising outcomes between two canopy levels, this comparison does not identify whether these responses come from canopy closure, successional status or environmental variables such as light exposure or drought.

5.2 Changes in trait expression driven by drought and successional status

Before comparing leaf traits with LAI, an investigation into how drought stress could impact trait responses was performed (Poorter et al., 2012; Poorter et al., 2009). To assess the impact of water stress, a comparison between five species in the drought and control sites of the upper canopy was made (Figure 5). Reduced water availability can have profound effects on plant function and morphology (Poorter et al., 2009). One response is to reduce stomatal conductance to inhibit water loss (Sperry, 2000), which ultimately increases the $\delta^{13}C$ of leaves as discrimination against ^{13}C is increased (Farquhar et al., 1989) This is not seen. LMA should also be affected, because leaf expansion is reduced under water stress (Poorter et al., 2009). Several recent studies have suggested that light may not be the primary driving force behind vertical gradients of LMA in forest canopies (Cavaleri et al., 2010; Meinzer et al., 2008; Burgess & Dawson, 2007). Instead, diminishing xylem pressure and cell turgor and are likely to be linearly related to height (Cavaleri et al., 2010). If LMA were responding to water availability, an impact on the mean values of LMA in the drought site as compared to the control could be expected, which is not seen (Figure 5b). A reduction in turgor pressure can also reduce cell expansion. If drought had an effect on traits, CA would

have been noticeably smaller (Witkowski & Lamont, 1991). This can also cause the same dry mass to being contained within a smaller leaf area, thus raising LMA (Witkowski & Lamont, 1991). UI is also expected to decrease in this instance, as decreased cell expansion inhibits the formation if cell wall curvature. None of the leaf traits measured support the hypothesis. No distinct change was seen in the drought treatment site (Figure 5). From these results, it is concluded that samples from the drought site in the upper canopy will not impact analysis of traits made against LAI, and thus these samples are retained in the subsequent analyses.

Individual trees beneath canopy gaps are subject to different exposure compared to those beneath closed canopies (Ellsworth & Reich, 1992), which can be reflected in leaf physiognomy. To investigate whether canopy gaps could impact the overall LAI gradient, a comparison between US-G and US-C samples was made (Figure 6). No discernible difference in $\delta^{13}C$, CA or UI value is seen. There is an increased range of LMA values within US-G, although its mean values are within the range of US samples. The data does not support the hypothesis that US-G traits will differ from those from US-C. A potential reason for this is that the gap may not be large enough to cause variance in these leaf traits. Niinemets et al. (2004) explains that it is not peak irradiance which determines the LMA of a plant, but that of the total photon irradiance integrated over the day. That is, as the gap is relatively small, sunlight only penetrates to the ground for a small period of the day. This small window of high-exposure would not be substantial enough to cause leaf variations (Niinemets et al., 2004). Furthermore, microhabitats within the gap may be introducing trait variance on an individual-tree scale (Ellsworth & Reich, 1992). No species displayed a change in $\delta^{13}C$ with variable

LAI, the exception being *E. microneura*, which has a large decrease in the $\delta^{13}C$ of leaves beneath the gap (Figure 6a). If the atmospheric accumulation of ^{12}C from decaying leaf litter were disturbed by atmospheric turbulence, it could be expected that all the species to increase in $\delta^{13}C$. A decrease in discrimination against ^{13}C can also be caused by increased photosynthesis under high radiant exposure (Ellsworth & Reich, 1992). Therefore, the individual *E. microneura* may be receiving higher sun-exposure than other species. Overall, because there is no consistent directional change, it is concluded that the gap has no effect on traits in the understory, and therefore US-G samples were included in the following analyses.

5.3 Quantifying traits with LAI gradients in a vertical profile

To test if the observed trends are controlled by canopy closure and the gradient of light, a further analysis was performed to investigate the effect of LAI (Figure 7). Systematic sampling from the UC to the US and LAI measurements enable a gradient of light to be quantified. If leaf traits are correlated with this light gradient, a linear response could be expected (Cavaleri et al., 2010). This hypothesis is supported. $\delta^{13}C$ displays a statistically significant linear correlation for four out of five of the species and an increasingly negative $\delta^{13}C$ with increasing LAI, supporting the "canopy effect" (Graham et al., 2014; Farquhar et al., 1989) (Figure 7a). The rate of change is also relatively consistent among species. Therefore, carbon isotopes have the potential to act as a proxy to be used in canopy reconstructions.

Previous modelling has identified that a minimum amount of 50 randomly sampled leaves is adequate for capturing the isotopic gradient of a rainforest (Graham et al., 2014). To test this theory, a regression was performed for all species correlated with

LAI (Figure 8). The results show a significant linear result which supports the model. Therefore, the non-significant response of *R. angustifolia* does not have an impact on the overall appearance of the isotopic gradient, and the "canopy effect" could be used to reconstruct LAI irrespective of fossil species assemblage.

LMA also correlates with LAI (Figure 7b). This supports the hypothesis that species beneath increased exposure (lower LAI), have a significantly increased LMA and aligns with previous studies (Coble & Cavaleri, 2015; Oguchi et al., 2005; Turney et al., 2002; Oberbauer & Strain, 1986), where leaves grown in high light had an increased LMA compared to those in the understory. Although the magnitude of responses changes with species, many show a similar directional change. *R. angustifolia* is the only species without a significant result. A meta-analysis by (Poorter et al., 2009) further displays the multiple causes of LMA variation in multiple ecosystems, and concludes that LMA varies strongly with light and has potential to act as a proxy for canopy structure, irrespective of species specific impacts.

CA showed a significant correlation with variable LAI in *C. myrianthus* and *M. globosa* (Figure 7c). *R. angustifolia* and *E. microneura* display no significant response. Although the response differs among species, the overall trend supports conclusions presented by Kürschner (1997), where distinct differences exist between sun-exposed and shaded leaves. This also supports the hypothesis that sun-exposed leaves would have smaller CA than shaded leaves.

Sun-exposed leaves undergo more rapid cuticle hardening, which reduces undulation (Kürschner, 1997). The hypothesis that only a portion of species would respond to LAI has been supported (Figure 7d). *E. microneura* and *M. globosa* are the only species with a statistically significant response. This is consistent with previous studies where UI decreases with increasing light (Bush et al., 2017; Dunn et al., 2015; Kürschner, 1997; Watson, 1942). It should be noted that while *M. globosa* is statistically significant, the change in UI is minimal (measurement variance 0.098) and is not useful for inferring light environment. It should be noted that UI was calculated from the abaxial cells for consistency with previous studies (Bush et al., 2017), which have neglected the upper epidermal features because the stomata are more present on the abaxial (lower) epidermis, which is another feature used to infer light environment (Xiao et al., 2011; Schoch et al., 1980). However, adaxial epidermal tissue has been found to be more sensitive to environmental change (Xiao et al., 2011). Although the adaxial epidermal cells were not used in this study, *M.globosa* had a noticeable difference between the two tissue types. While there was no response in abaxial cells, undulation was prominent in adaxial cells (Figure 12). This has implications for using this proxy on fossils. Incomplete fossils therefore require identification of species and of the cuticle side.

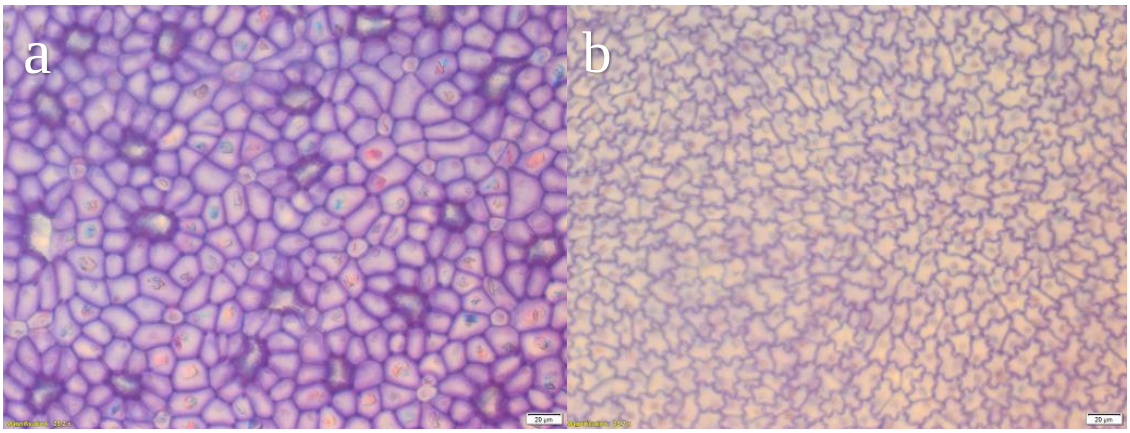

Figure 12: Images of the (a) abaxial (lower) and (b) adaxial (upper) epidermal material of *M. globosa* from the IC of the control site. Images are taken under 25.2x magnification, scale is 20 µm. Average UI of adaxial cells: 1.09. Average UI of abaxial cells: 1.32.

Future studies which quantify differences between adaxial and abaxial leaf tissues will therefore be beneficial for calibrating proxies.

5.4 Reconstructing LMA from petiole width and leaf area

The model of petiole width scaled by leaf area to predict LMA, produced by Royer et al., (2007), has been tested to determine if this data would produce a linear correlation to measured LMA (Figure 9). These traits were expected to be closely related because the petiole is required for the mechanical support of the leaf (Royer et al., 2007; Chazdon, 1986). Although the relationship between PW^2/A and LMA of is not statistically significant, nor does it produce a linear trend, it does lie within the prediction intervals of the original study (Royer et al., 2007). Perhaps it is unrealistic to expect a replication of the distribution which came from geographically widespread and climactically diverse sites, whereas species from this study came from a single tropical rainforest. Rather, the clumped distribution of the data from a single environment is showing an average of that environment. If this model were applied to the average LMA range of a fossil assemblage, although it does lack a linear trend and therefore could not be used to characterise variables within a forest, it could be used predict the habitat. In tropical rainforests, the average range of LMA lies between approximately 50 to 120 g/m^2 (Poorter et al., 2009), consistent with the predicted and measured LMA distribution. Values which lie either side of this, may be indicative of other habitats such as grasslands (approximate average LMA: 30 – 70 g/m^2) or woodlands (approximate average LMA: 80 – 220 g/m^2) (Poorter et al., 2009). A further examination into the LMA distribution within the ecosystem was highlighted by forest level separation (Figure 9). There was no difference between the predicted LMA of UC and US samples, therefore this proxy cannot be used to infer conditions within a forest

but has the potential to illustrate the average LMA of an ecosystem. While no significant result was found in petiole width, petiole length has also found to correlate with leaf shape and environmental conditions (Falster & Westoby, 2003; Givnish & Vermeij, 1976).

5.5 Between trait correlations

Identifying multiple leaf traits that correlate with LAI will enable accurate reconstructions of canopy closure because co-varying measurements will be able to re-confirm the inferred light environment. Out of thirteen comparisons of traits with all species combined, only four had statistically significant correlations (Figure 10). Higher CA correlated with increased UI, in Figure 10d, represents a mechanism which could be used to infer light environment within forests. Increased cell wall thickness and decreased cell expansion could account for the decrease in UI, since the curvature is not able to develop with reduced growth (Witkowski & Lamont, 1991). Another result of decreased cell size is a higher count of epidermal cells, leading to approximately the same dry mass being contained within a smaller leaf area (Witkowski & Lamont, 1991). Both UI and CA have a significant linear response with LMA (Figure 10b and 10c), suggesting that a probable cause of increased LMA is due to an increase in cell density. It is proposed that CA and UI in addition to inferring LAI, could be used predict LMA of forests from leaf fossil assemblages. This is beneficial, because LMA is a central ecological trait that cannot be directly measured from the fossil record (Royer et al., 2007).

$\delta^{13}C$ also had a significant correlation with LMA (Figure 10a), showing that both these traits reflect canopy closure. Furthermore, the trend in $\delta^{13}C$ values display a distinct

separation of plotted values from the UC, IC and US which the others do not. Therefore, these correlations could be used to predict the internal structure of forests.

5.6 Implications for palaeoecology

Our understanding of past environments, their light conditions, humidity and atmospheric composition is reliant on the accuracy with which the internal architecture of those ecosystems can be reconstructed. Identifying the type of past ecosystems from the fossil record can inform us about larger-scale processes, such as climate and regional rainfall distribution (Graham *et al.*, 2014). Closed canopy forests can be recognised in fossils because of their characteristic light gradient, which causes large spatial variation in leaf traits within the forest. Therefore, fossil assemblages also contain this variability. If these leaf traits can be characterised beyond simple sun and shade morphotypes, and correlated with these LAI gradients, we can explain the variability found in fossil records and understand the three-dimensional structure of past vegetation (Mosbrugger et al., 1994).

Past research has highlighted the great control that light has on leaf traits (Coble & Cavaleri, 2015; Graham et al., 2014; Xiao et al., 2011; Markesteijn et al., 2007; D. S. Ellsworth & Reich, 1993). Graham et al., (2014) has demonstrated how $\delta^{13}C$ correlates with light gradients within rainforests. Xiao et al. (2011) used UI, CA and cell density to determine differences between sun and shade leaves. Dunn et al., (2015) has further used a correlation between UI and light on fossils to infer vegetation changes, climate and reconstruct LAI from fossil specimens of Patagonia from the Cenozoic. These results are promising, and have broadened our knowledge about past ecological systems

and canopy structure. Traits from leaf samples from the Daintree Rainforest have confirmed that UI, LMA, CA and $\delta^{13}C$ can be strong predictors of canopy closure.

LMA is a useful measure of ecological adaptations linking to nutrient availability, water status and climate (Royer et al., 2007). It also cannot be directly measured from the fossil record. Therefore, the ability to predict LMA of fossils would greatly enhance internal forest reconstructions. Though petiole width scaling could not predict LMA in the Daintree Rainforest, UI and CA have significant relationships with measured LMA. These proxies are further beneficial because they require only a portion of a fossilized leaf to reconstruct forest canopy closure. However, UI is species specific, and should be used with caution. Calibrations made on extant species or living relatives will ensure accuracy in predictions from UI. The comparison between understory samples from beneath a gap and canopy samples within a drought did not impact leaf traits. Therefore, gaps in canopy closure do not impact total canopy reconstruction. Further examination into the role of LAI on traits and additional proxies to predict LMA will be beneficial. Continued comparisons of fossil taxa with modern analogues will be also important to ensure the most accurate information is attained from fossils (Mosbrugger et al., 1994).

6. CONCLUSIONS

Analysis of leaf traits with LAI have displayed significant responses in $\delta^{13}C$, LMA, CA and UI. This suggests they can be used as proxies to infer LAI, however, responses were variable among species. The most variation in UI was seen in *Calamus australis* and *Hypserpa decumbens. Myristica globosa* and *Cleistanthus myrianthus* displayed no measurable difference between the US and UC in the rainforest. Therefore, UI should be used with caution and fossil taxa should be calibrated to extant examples or relatives

to ensure that this proxy is appropriate for use on that species. Neither drought conditions nor the presence of a gap in canopy closure had a significant impact on traits. The non-significant response in $\delta^{13}C$ of one species did not impact the overall $\delta^{13}C$ gradient. $\delta^{13}C$, is therefore a reliable proxy for inferring canopy conditions of closed canopy forests.

Petiole width and leaf area did not predict the internal LMA distribution of the rainforest. However, the average distribution was within the average LMA of a rainforest. This model can therefore be used for inferring habitat type. Alternate leaf traits such as CA, UI and $\delta^{13}C$ did correlate with LMA. As LMA is such an integral component of ecological functions, the internal structure of rainforests could be determined from these traits instead.

Since responses were variable in all analyses between species, there is a need to acquire a better understanding of how multiple species react to different light environments in both tropical and temperate forests. This research has established the base of a multi-proxy tool that could be used on closed canopy rainforests worldwide. The study design could be applied to other closed canopy ecosystems to investigate how the controls vary in different climactic zones. This would form a comprehensive understanding of the role that closed canopies have on leaf trait variability and consequently enable more accurate canopy reconstructions.

7. ACKNOWLEDGMENTS

I would like to extend my gratitude to my primary supervisor Dr. Cesca McInerney, for granting me so much of her time, guidance and continued support throughout this project. To Dr. Lucas Cernusak, for sharing his wealth of knowledge and advice throughout the year. To Dr. Alexander Cheesman, for his outstanding support in the field and continued assistance. Thank you to The Environmental Institute at The University of Adelaide for their generous financial support, which enabled the completion of this research. The JCU Daintree Rainforest Observatory and Dr. Susan Laurance, for allowing us to undertake this research in such a phenomenal research facility. Also to Christina Macdonald and the Terrestrial Ecosystem Research Network, for lending the LAI-2200. I thank Dr. Katheryn Hill for helping me in the laboratory. Also to Myall Tarran, for saving my leaves when cuticles started falling apart! A very big thank you to Mark Rollog, for processing samples for carbon isotope values so quickly. Also Siân Howard, for her advice on written work and laboratory techniques. Finally, I would like to thank Mathew Raven, Claire Murphy and members of Cesca's lab group for their support this year.

REFERENCES (LEVEL 1 HEADING)

BELLINGHAM, P. J. (1991). Landforms Influence Patterns of Hurricane Damage: Evidence From Jamaican Montane Forests. *Biotropica, 23*(4), 427-433. doi: 10.2307/2388262

BOYCE, C., LEE, J.-E., S. FEILD, T., BRODRIBB, T., & A. ZWIENIECKI, M. (2010). *Angiosperms Helped Put the Rain in the Rainforests: The Impact of Plant Physiological Evolution on Tropical Biodiversity1* (Vol. 97).

BURGESS, S. S. O., & DAWSON, T. E. (2007). Predicting the limits to tree height using statistical regressions of leaf traits. *New Phytologist, 174*(3), 626-636. doi: 10.1111/j.1469-8137.2007.02017.x

BUSH, R. T., WALLACE, J., CURRANO, E. D., JACOBS, B. F., MCINERNEY, F. A., DUNN, R. E., & TABOR, N. J. (2017). Cell anatomy and leaf δ13C as proxies for shading and canopy structure in a Miocene forest from Ethiopia. *Palaeogeography, Palaeoclimatology, Palaeoecology*. doi: https://doi.org/10.1016/j.palaeo.2017.07.015

CAVALERI, M. A., OBERBAUER, S. F., CLARK, D. B., CLARK, D. A., & RYAN, M. G. (2010). Height is more important than light in determining leaf morphology in a tropical forest. *Ecology, 91*(6), 1730-1739. doi: 10.1890/09-1326.1

CHAZDON, R. L. (1986). The Costs of Leaf Support in Understory Palms: Economy Versus Safety. *The American Naturalist, 127*(1), 9-30. doi: 10.1086/284464

CHRISTOPHEL, D. C., & GREENWOOD, D. R. (1989). Changes in climate and vegetation in Australia during the tertiary. *Review of Palaeobotany and Palynology, 58*(2), 95-109. doi: http://dx.doi.org/10.1016/0034-6667(89)90079-1

COBLE, A. P., & CAVALERI, M. A. (2015). Light acclimation optimizes leaf functional traits despite height-related constraints in a canopy shading experiment. *Oecologia, 177*(4), 1131-1143. doi: 10.1007/s00442-015-3219-4

COSTION, C. M., EDWARDS, W., FORD, A. J., METCALFE, D. J., CROSS, H. B., HARRINGTON, M. G., . . . CRAYN, D. M. (2015). Using phylogenetic diversity to identify ancient rain forest refugia and diversification zones in a biodiversity hotspot. *Diversity and Distributions, 21*(3), 279-289. doi: 10.1111/ddi.12266

CROWLEY, B. E., MCGOOGAN, K. C., & LEHMAN, S. M. (2012). Edge Effects on Foliar Stable Isotope Values in a Madagascan Tropical Dry Forest. *PLOS ONE, 7*(9), e44538. doi: 10.1371/journal.pone.0044538

DENSLOW, J. S. (1980). Gap partitioning among tropical rainforest trees. *Biotropica*, 47-55.

DETTMANN, M. (1994). Cretaceous vegetation: the microfossil record. *History of the Australian vegetation: Cretaceous to Recent*, 143-170.

DILCHER, D. L. (1974). Approaches to the identification of angiosperm leaf remains. *The Botanical Review, 40*(1), 1-157. doi: 10.1007/bf02860067

DRAGOVICH, D., & GROSE, J. (1990). Impact of tourists on carbon dioxide levels at Jenolan Caves, Australia: an examination of microclimatic constraints on tourist cave management. *Geoforum, 21*(1), 111-120. doi: https://doi.org/10.1016/0016-7185(90)90009-U

DUNN, R. E., STRÖMBERG, C. A. E., MADDEN, R. H., KOHN, M. J., & CARLINI, A. A. (2015). Linked canopy, climate, and faunal change in the Cenozoic of Patagonia. *Science, 347*(6219), 258-261. doi: 10.1126/science.1260947

ELLSWORTH, & REICH, P. B. (1992). Leaf mass per area, nitrogen content and photosynthetic carbon gain in Acer saccharum seedlings in contrasting forest light environments. *Functional Ecology*, 423-435.

ELLSWORTH, D. S., & REICH, P. B. (1993). Canopy structure and vertical patterns of photosynthesis and related leaf traits in a deciduous forest. *Oecologia, 96*(2), 169-178. doi: 10.1007/bf00317729

FALSTER, D. S., & WESTOBY, M. (2003). Leaf size and angle vary widely across species: what consequences for light interception? *New Phytologist, 158*(3), 509-525.

FAO. (1999) *State of the World's Forests*: Food and Agriculture Organization of the United Nations, Rome.

FARQUHAR, G. D., EHLERINGER, J. R., & HUBICK, K. T. (1989). Carbon isotope discrimination and photosynthesis. *Annual review of plant biology, 40*(1), 503-537.

GARTEN, C., & TAYLOR, G. (1992). Foliar δ 13 C within a temperate deciduous forest: spatial, temporal, and species sources of variation. *Oecologia, 90*(1), 1-7.

GIVNISH, T. J., & VERMEIJ, G. J. (1976). Sizes and Shapes of Liane Leaves. *The American Naturalist, 110*(975), 743-778. doi: 10.1086/283101

GRAHAM, H. V., PATZKOWSKY, M. E., WING, S. L., PARKER, G. G., FOGEL, M. L., & FREEMAN, K. H. (2014). Isotopic characteristics of canopies in simulated leaf assemblages. *Geochimica et Cosmochimica Acta, 144*, 82-95. doi: http://doi.org/10.1016/j.gca.2014.08.032

GREENWOOD, D., & C CHRISTOPHEL, D. (2005). *The origins and Tertiary history of Australian "Tropical" rainforests*.

GROVE, S. J., TURTON, S. M., & SIEGENTHALER, D. T. (2000). Mosaics of canopy openness induced by tropical cyclones in lowland rain forests with contrasting management histories in northeastern Australia. *Journal of Tropical Ecology, 16*(6), 883-894.

HILL, R. S. (2004). Origins of the southeastern Australian vegetation. *Philosophical Transactions of the Royal Society of London B: Biological Sciences, 359*(1450), 1537-1549.

HOLLINGER, D. (1989). Canopy organization and foliage photosynthetic capacity in a broad-leaved evergreen montane forest. *Functional Ecology*, 53-62.

INC., L.-C. (2010). *LAI-2200 Plant Canopy Analyzer: Instruction Manual*. Lincoln, Nebraska 68504, USA.

JACKSON, P. C., MEINZER, F. C., GOLDSTEIN, G., HOLBROOK, N. M., CAVELIER, J., & RADA, F. (2012). Environmental and physiological influences on carbon isotope composition of gap and understory plants in a lowland tropical forest. *Stable isotopes and plant carbon-water relations*, 131.

JACQUES, E., HECTORS, K., GUISEZ, Y., PRINSEN, E., JANSEN, M. A. K., VERBELEN, J.-P., & VISSENBERG, K. (2011). UV radiation reduces epidermal cell expansion in Arabidopsis thaliana leaves without altering cellular microtubule organization. *Plant Signaling & Behavior, 6*(1), 83-85. doi: 10.4161/psb.6.1.14127

JORDAN, G. J., CARPENTER, R. J., & BRODRIBB, T. J. (2014). Using fossil leaves as evidence for open vegetation. *Palaeogeography, Palaeoclimatology, Palaeoecology, 395*, 168-175.

JUENGER, T. E., MCKAY, J. K., HAUSMANN, N., KEURENTJES, J. J. B., SEN, S., STOWE, K. A., . . . RICHARDS, J. H. (2005). Identification and characterization of QTL underlying whole-plant physiology in Arabidopsis thaliana: δ13C, stomatal conductance and transpiration efficiency. *Plant, Cell & Environment, 28*(6), 697-708. doi: 10.1111/j.1365-3040.2004.01313.x

JUPP, D. L. B., CULVENOR, D. S., LOVELL, J. L., NEWNHAM, G. J., STRAHLER, A. H., & WOODCOCK, C. E. (2009). Estimating forest LAI profiles and structural parameters using a ground-based laser called 'Echidna®☆. *Tree Physiology, 29*(2), 171-181. doi: 10.1093/treephys/tpn022

JURIK, T. W. (1986). Temporal and Spatial Patterns of Specific Leaf Weight in Successional Northern Hardwood Tree Species. *American Journal of Botany, 73*(8), 1083-1092. doi: 10.2307/2443788

KERP, H. (1990). The Study of Fossil Gymnosperms by Means of Cuticular Analysis. *PALAIOS, 5*(6), 548-569. doi: 10.2307/3514861

KÜRSCHNER, W. M. (1997). The anatomical diversity of recent and fossil leaves of the durmast oak (Quercus petraea Lieblein/Q. pseudocastanea Goeppert) — implications for their use as biosensors of palaeoatmospheric CO2 levels. *Review of Palaeobotany and Palynology, 96*(1), 1-30. doi: http://dx.doi.org/10.1016/S0034-6667(96)00051-6

LAURANCE, S. (2015) *A Raincoat for A Rainforest*. Australian Science (Vol 9).

LOCKHEART, M., POOLE, I., VAN BERGEN, P., & EVERSHED, R. (1998a). Leaf carbon isotope compositions and stomatal characters: important considerations for palaeoclimate reconstructions. *Organic Geochemistry, 29*(4), 1003-1008.

LOCKHEART, M. J., POOLE, I., VAN BERGEN, P. F., & EVERSHED, R. P. (1998b). Leaf carbon isotope compositions and stomatal characters: important considerations for palaeoclimate reconstructions. *Organic Geochemistry, 29*(4), 1003-1008. doi: https://doi.org/10.1016/S0146-6380(98)00168-5

MARKESTEIJN, L., POORTER, L., & BONGERS, F. (2007). Light-dependent leaf trait variation in 43 tropical dry forest tree species. *American Journal of Botany, 94*(4), 515-525.

MEDINA, E., & MINCHIN, P. (1980). *Stratification of ?13C values of leaves in Amazonian rain forests* (Vol. 45).

MEINZER, F. C., BOND, B. J., & KARANIAN, J. A. (2008). Biophysical constraints on leaf expansion in a tall conifer. *Tree Physiology, 28*(2), 197-206.

MOSBRUGGER, V., GEE, C. T., BELZ, G., & ASHRAF, A. R. (1994). Three-dimensional reconstruction of an in-situ Miocene peat forest from the Lower Rhine Embayment, northwestern Germany—new methods in palaeovegetation analysis. *Palaeogeography, Palaeoclimatology, Palaeoecology, 110*(3), 295-317. doi: https://doi.org/10.1016/0031-0182(94)90089-2

NIER, A. O., & GULBRANSEN, E. A. (1939). Variations in the relative abundance of the carbon isotopes. *Journal of the American Chemical Society, 61*(3), 697-698.

NIINEMETS, KULL, O., & TENHUNEN, J. D. (2004). Within-canopy variation in the rate of development of photosynthetic capacity is proportional to integrated quantum flux density in temperate deciduous trees. *Plant, Cell & Environment, 27*(3), 293-313. doi: 10.1111/j.1365-3040.2003.01143.x

NIINEMETS, Ü. (2001). GLOBAL-SCALE CLIMATIC CONTROLS OF LEAF DRY MASS PER AREA, DENSITY, AND THICKNESS IN TREES AND SHRUBS. *Ecology, 82*(2), 453-469. doi: 10.1890/0012-9658(2001)082[0453:GSCCOL]2.0.CO;2

O'LEARY, M. H. (1981). Carbon isotope fractionation in plants. *Phytochemistry, 20*(4), 553-567. doi: http://dx.doi.org/10.1016/0031-9422(81)85134-5

OBERBAUER, S. F., & STRAIN, B. R. (1986). Effects of Canopy Position and Irradiance on the Leaf Physiology and Morphology of Pentaclethra macroloba (Mimosaceae). *American Journal of Botany, 73*(3), 409-416. doi: 10.2307/2444084

OGUCHI, R., HIKOSAKA, K., & HIROSE, T. (2005). Leaf anatomy as a constraint for photosynthetic acclimation: differential responses in leaf anatomy to increasing growth irradiance among three deciduous trees. *Plant, Cell & Environment, 28*(7), 916-927. doi: 10.1111/j.1365-3040.2005.01344.x

P. TRENERRY, M., F. LAURANCE, W., & R. MCDONALD, K. (1994). Further evidence for the precipitous decline of endemic rainforest frogs in tropical Australia*. *Pacific Conservation Biology, 1*(2), 150-153. doi: https://doi.org/10.1071/PC940150

POORTER, H., NIINEMETS, Ü., POORTER, L., WRIGHT, I. J., & VILLAR, R. (2009). Causes and consequences of variation in leaf mass per area (LMA): a meta-analysis. *New Phytologist, 182*(3), 565-588. doi: 10.1111/j.1469-8137.2009.02830.x

POORTER, H., NIKLAS, K. J., REICH, P. B., OLEKSYN, J., POOT, P., & MOMMER, L. (2012). Biomass allocation to leaves, stems and roots: meta-analyses of interspecific variation and environmental control. *New Phytologist, 193*(1), 30-50. doi: 10.1111/j.1469-8137.2011.03952.x

ROYER, L. D., SACK, L., WILF, P., & CARIGLINO, B. (2007). Fossil leaf economics quantified: calibration, Eocene case study, and implocations. *Paleobiology, 33*(4), 574-589. doi: https://doi.org/10.1666/07001.1

RSCQ. (1986) Tropical Rainforests of North Queensland: Their Conservation Significance. *Special Australian Heritage Publication Series*. Canberra: Australian Government Publishing Service.

SCHOCH, P.-G., ZINSOU, C., & SIBI, M. (1980). Dependence of the Stomatal Index on Environmental Factors during Stomatal Differentiation in Leaves of Vigna sinensis L.1. EFFECT OF LIGHT INTENSITY. *Journal of Experimental Botany, 31*(5), 1211-1216. doi: 10.1093/jxb/31.5.1211

SOKAL, R. R., & ROHLF, F. J. (1981). Biometry: the principles and practice of statistics in biological research 2nd edition.

SPERRY, J. S. (2000). Hydraulic constraints on plant gas exchange. *Agricultural and Forest Meteorology, 104*(1), 13-23. doi: https://doi.org/10.1016/S0168-1923(00)00144-1

TURNEY, C. S., HUNT, J. E., & BURROWS, C. (2002). Deriving a consistent δ13C signature from tree canopy leaf material for palaeoclimatic reconstruction. *New Phytologist, 155*(2), 301-311.

VAN DER MERWE, N. J., & MEDINA, E. (1989). Photosynthesis and 13C12C ratios in Amazonian rain forests. *Geochimica et Cosmochimica Acta, 53*(5), 1091-1094. doi: https://doi.org/10.1016/0016-7037(89)90213-5

VAN DER MERWE, N. J., & MEDINA, E. (1991). The canopy effect, carbon isotope ratios and foodwebs in amazonia. *Journal of Archaeological Science, 18*(3), 249-259. doi: http://dx.doi.org/10.1016/0305-4403(91)90064-V

VANDERWAL, J., SHOO, L. P., & WILLIAMS, S. E. (2009). New approaches to understanding late Quaternary climate fluctuations and refugial dynamics in Australian wet tropical rain forests. *Journal of Biogeography, 36*(2), 291-301. doi: 10.1111/j.1365-2699.2008.01993.x

WAGNER-CREMER, F., FINSINGER, W., & MOBERG, A. (2010). Tracing growing degree-day changes in the cuticle morphology of Betula nana leaves: a new micro-phenological palaeo-proxy. *Journal of Quaternary Science, 25*(6), 1008-1017. doi: 10.1002/jqs.1388

WATSON, R. W. (1942). THE MECHANISM OF ELONGATION IN PALISADE CELLS. *New Phytologist, 41*(3), 206-221. doi: 10.1111/j.1469-8137.1942.tb07074.x

WITKOWSKI, E. T. F., & LAMONT, B. B. (1991). Leaf specific mass confounds leaf density and thickness. *Oecologia, 88*(4), 486-493. doi: 10.1007/bf00317710

WRIGHT, I. J., REICH, P. B., WESTOBY, M., & ACKERLY, D. D. (2004). The worldwide leaf economics spectrum. *Nature, 428*(6985), 821.

XIAO, L., SUN, B., LI, X., REN, W., & JIA, H. (2011). Anatomical variations of living and fossil Liquidambar leaves: A proxy for paleoenvironmental reconstruction. *Science China Earth Sciences, 54*(4), 493-508. doi: 10.1007/s11430-010-4135-4

ZHAO, L., XIAO, H., & LIU, X. (2006). Variations of foliar carbon isotope discrimination and nutrient concentrations in Artemisia ordosica and Caragana korshinskii at the southeastern margin of China's Tengger Desert. *Environmental Geology, 50*(2), 285. doi: 10.1007/s00254-006-0209-1

APPENDIX A: EXTENDED METHODS

Study area

All samples were obtained from the James Cook University research facility within the Daintree Rainforest, which is situated on the low-land coastal plains of the Daintree rainforest. In 1998, an official, permanent study site was established with a construction crane that enables access to approximately 0.95ha of rainforest canopy (Stork, 2007). A permanent drought study site also exists under the crane's reaches, run by Associate Professor Susan Lawrence, James Cook University, College of Science and Engineering. The location of the study site was chosen for its high biodiversity and

conservation values and because it had not undergone logging in recent times (Stork, 2007).

Upper canopy and understory samples

Samples were obtained from the James Cook University Daintree Rainforest Observatory, situated on the low-land coastal plains of the Daintree rainforest. Samples of 15 species were taken for analysis at The University of Adelaide in July 2017 from the understory and upper canopy, along with LAI measurements. For species comparison between rainforest levels, fully sun-lit upper canopy samples and associated $\delta^{13}C$, LMA, leaf area and petiole measurements were supplied by Dr Alex Cheesman, James Cook University, College of Science and Engineering (centre for Tropical Environmental and Sustainability Studies). Understory samples were supplied by Dr Lucas Cernusak, James Cook University, College of Science and Engineering (centre for Tropical Environmental and Sustainability Studies) in May 2017. These samples were analysed at The University of Adelaide.

Field definitions

Leaves from five species (*Argyrodendron peralatum, Myristica globosa ssp. muelleri, Endiandra microneura, Cleistanthus myrianthus* and *Rockinghamia angustifolia*) were selected because of their commonality within all heights and areas of the study area. A simple height and LAI comparison across several sites was initially planned, however, it was found that this would not suffice due to the complexities of rainforest vegetation structure. The heterogeneous canopy crown is caused by a combination of damage from frequent storm activity and a range of gap regeneration strategies which allows

communities of various ages and growth rates to create a mosaic of vegetation heights and densities (Webb, 1958; Denslow, 1980). This variability enables areas to exist between the understory and upper canopy which are neither fully exposed or directly under foliage. They cannot be defined as upper crown because they have surrounding vegetation on either side, and they can still be exposed to full sunlight for a portion of the day. Three site levels (which do not have distinct heights) were identified in a vertical gradient from the canopy to the understory to capture this variability. These levels were the upper crown (UC, fully exposed), inner canopy (IC, partial cover by surrounding vegetation but not overhanging foliage) and the understory (US, closed canopy, 40% or more cover by foliage (FAO, 1999)). In addition to the closed canopy understory site (US-C), samples were also taken from beneath a significant canopy gap (Gap understory, US-G) to introduce light variation at ground level. Leaves were also sampled from the UC and ICIC levels within the drought experiment site (upper canopy drought (UC_D), interior canopy drought (IC-D)).

Sampling procedure

A total of ten trees were selected for canopy sampling, which were made accessible by the Daintree Rainforest Observatory's construction crane. An additional sample set of all five species were taken from UC and IC levels within the drought experiment. Each sample consisted of six leaves, and two samples were taken from each tree, one from UC and one from IC. Leaves that were sampled were selected on the basis that they stemmed from the same branch and displayed minimal insect damage. Along with LAI, the position of each sample on its tree was measured using a compass. Height was also measured by placing a weight on a field tape measure and lowering it to the ground.

Understory samples were taken from two sites accessible by foot. The first site was beneath a closed canopy, defined by 40% or more cover by overhanging foliage (FAO, 1999). The second site was beneath a significant gap in the canopy. This area was dominated by young growth under high-exposure. At least one sample per species was taken from each site and each sample point was tagged for future reference. Only 3 leaves were taken per sample in the understory because many individuals were young and did not have excess foliage. At each sample a single LAI measurement was taken.

Leaf Area Index (LAI)

The leaf area index (LAI) is a method which assesses the degree of canopy gap fraction, or the amount of sky visible beneath a canopy at sampling point. A Licor LAI-2200 was used to record the foliage cover at each sample point This estimated the amount of leaf surface area by comparing a fully exposed above canopy reading (A reading) with a measurement adjacent to each sample point (B reading). The LAI-2200 has been designed primarily for quantifying LAI over an entire field, and multiple measurements over transects are recommended. As this study aimed to characterise the variability above a single point in the rainforest, a single measurement was taken adjacent to each leaf sample point. All canopy samples (UC and IC) were measured before noon when the sun was lowest. Each LAI calculation consisted of an A reading and accompanying B reading. Unfortunately, cloud cover was not consistent throughout the morning of light measurements. Therefore, to make LAI as accurate as possible, a fully exposed reading (A reading) was made above the canopy crown immediately following the two leaf sampling points in the UC and IC of a single tree (B reading). The LAI-2200 wand was consistently orientated northward and an 180^{o} cap used to cover the eastern portion

of the sensor, to reduce the impact of direct sunlight.

Single LAI measurements were also taken adjacent to each understory sample in a single afternoon. As per the LAI-2200 manual, A readings were taken in a clear, open field adjacent to the rainforest prior to B readings to reduce surrounding vegetation from impeding the sensor view, named LAI US data set 1. However, A readings were not taken as frequently as suggested (following each B reading) because the understory sites were not easily accessible. Therefore, the time taken between A and B readings was of concern because cloud cover could change rapidly, which could generate a false difference between the two readings and calculate LAI incorrectly. A second set of light measurements (LAI US data set 2) was taken before dusk, after the surrounding mountains blocked direct sunlight. Cloud cover was also more consistent during this time. One single A reading was taken before and after all B measurements. In this data set, all B measurements were also taken within a shorter time period because samples had already been taken, thus reducing the amount of variation created by moving cloud cover.

LAI Data Processing

Recorded data was processed through the LAI-2200 associated program, FV2200, to calculate LAI for the three data sets. These data sets were the upper canopy, LAI US data set 1 and LAI US data set 2. As LAI data set 2 measurements were taken in a shorter time period and under more consistent cloud conditions, this set was used to characterise the exposure of understory samples. LAI was also calculated in two different ways to test how using different A and B reading comparisons could impact

LAI. The first calculated LAI from the single closest A reading to each B reading in time. The second method interpolated from the closest A reading in time before and after each B reading. Given that closest number did not calculate new values between readings where cloud cover could have changed, the LAI calculated from the closest A in time was used for further analysis. The LAI-2200 quantifies LAI using 5 zenith rings to measure a hemispherical view. A readings, being fully exposed, should have a lower LAI than any B readings. However, some A measurements were lower than the B reading in the outermost ring. This difference in attributed to interference from the surrounding mountains or the crane boom. To correct LAI, the outermost ring was removed from comparison as advised by the LAI-2200 manual.

Sample Sorting

All upper canopy samples contained six leaves per sample. Each set of leaves was sorted by increasing size and separated into two groups systematically to ensure an approximate gaussian distribution of leaf sizes in each group. One group was used for cuticle clearing and UI and the other for LMA. As understory samples only contained three leaves each, UI and LMA was calculated from the same leaf.

Fresh leaf sections were cut from each sample before drying and to ensure an accurate measurement of leaf mass could still be made, two leaf sections of (38.48mm^2 mm2) were removed from each understory leaf. One from approximately identical leaf tissue, along the blade margin where no significant vein structures or insect damage were present. One sample was analysed for UI and the other for drying.

Undulation Index (UI) and Cell Area

Species comparison samples

Each sample consisted of three leaves. From the right side of each leaf margin, half way between the blade top and base a ~1cm^2 section of fresh leaf material was cut. Leaf material was then placed into test tubes with a solution of 35% hydrogen peroxide and 65% ethanol. Test tubes were then placed into beakers of water and heated on a hot plate at approximately 75^{o}C for a minimum of 12 hours to clear the mesophyll tissue from the epidermis. Once cuticles became opaque, the dilute hydrogen peroxide was pipetted into a waste container and the test tubes were filled with water. Cuticles were then cleared of excess mesophyll and epidermal cells using a paintbrush in a small Petri dish. The cuticles were then dyed using crystal violet, and rinsed in two baths of ethanol followed by one of water. Dyed cuticles were then mounted on glass slides with heated glycerine jelly and allowed to set for a minimum of three hours. Photographs of the abaxial side (identified by the highest count of stomatal cells) were taken with an Olympus AX70 under 40x magnification. Three photographs per sample were taken and five well-preserved cells per photograph were traced in ImgJ, which measured the cell perimeter and area. In slides where there was little epidermis intact, multiple images were taken and a minimum of 15 abaxial cells were traced. The selection of cells were based on the premise they were not immediately adjacent to stomatal or guard cells and no cells next to to a previously traced cell were traced to eliminate the joining wall being traced twice. Cells that were associated with vein structures, which bare a structured arrangement, were not included. The measure of undulation was calculated by the following:

$$UI = \frac{C_e}{C_0} = \frac{C_e}{2 \times \pi x \sqrt{\frac{A_e}{\pi}}}$$

where C_e (µm) is the circumference of the cell, C_0 is the circumference of a circle with the same area as the cell and A_e (µm^2) is the area of the cell (Kürschner, 1997).). To determine the measurement error in UI, a single cell was traced 15 times. For a cell with an average UI of 1.05, the range in UI was 0.038. As this range was small, subsiquent analysis were performed by tracing each cell once. The average UI of all three leaves for each sample was used in subsiquent analysis.

Alternate clearing method

A high proportion of cuticles cleared for mounting on slides failed to yield adequate amounts of intact cuticle. These samples (predominantly *Argyrodendron peralatum*, *Cleistanthus myrianthus* and *Myristica globosa ssp. muelleri*) were put through an alternative clearing solution of 20% chromic acid, placed in a fume hood and left for a minimum of 24 hours. Cuticles were not put through the dying process because the chromic acid stained the cells. Each sample was then mounted and processed in the same manner.

Leaf mass per area (LMA)

Leaves were scanned using an office scanner to create images of 600x600 dpi that were processed through ImgJ. A single image with the same resolution of a ruler was used to set the scale (235 pixels/cm). A single calibration was used for the scale all images. Images were then converted to binary form to remove colour from leaf surface and the wand tool was used to trace the leaf margin. ImgJ then calculated the leaf area and

perimeter. Any parts of the leaf which were missing from damage were removed from area calculations. Leaf area was then converted from mm2 to m2.

After area calculations, three leaves from each upper canopy sample then dried in an oven for a minimum of 37 hours at 60^{o}C. Dried material was weighed on a Sartorius R200D in grams.

Understory samples which only had material removed for UI had a small 38.48mm^2 section which was weighed and multiplied by two. Samples which had more than one ---section removed was multiplied by the appropriate amount to replace missing leaf mass. The total leaf weight was then calculated by adding the total missing weight and the leaf weight. LMA was then calculated by the following:

$$LMA = mass/area$$

Where LMA = g/m^2 , mass in grams and area is in m^2. As each sample contained three leaves, the average of these were used in subsequent analysis.

Carbon Isotope Analysis

Leaf material was ground with a Retsch MM 400 Mixer Mill for a minimum of one minute for analysis of carbon isotopes. One half of each dried leaf was used for isotope analysis to ensure all tissue types were incorporated, and one half would remain available for future analysis. Each sample was homogenised by grinding one half of each three leaves in the same capsule. Between samples, these capsules were scrubbed with a dilute concentration of detergent and rinsed under deionised water three times. In a fume hood, these were then rinsed three times each with firstly methanol, then dichloromethane and finally n-hexane. Any equipment which was used during the grinding stage to scoop or scrape leaf material also underwent the cleaning process.

Approximately 2µg of ground leaf material was weighed into tin boats. Three standards were also run with the analysis in accordance with a sample run sheet supplied by Mark Rollog at The University of Adelaide. Target weights for each were: 2.5µg Glycene, 1µg Glutamic and 0.5µg TBA. Leaf samples were analysed for $\delta^{13}C$ with a EuroVector EuroEA elemental analyser, in line with a Nu Horizon CF-IRMS by Mark Rollog, at The University of Adelaide.

Data Analysis

A statistical program, GraphPad Prisim, was used to analyse relevant data used in this study. Each trait ($\delta^{13}C$, LMA, Cell area and UI value) was presented as a straight within species comparison between the US and UC. To display variance between the traits taken from the drought UC and control UC, an unpaired t-test was performed for each leaf trait to attain P-value and r^2. Parametric test assumed a gaussian distribution. The same data analysis was performed on differences between the gap and understory samples. A linear regression was performed for each trait by species against LMA.

Petiole width & LMA predictions

Petiole height and width measurements (mm) were made with a micrometer. These measurements were taken at the base of the leaf, where the two sides of the leaf blade terminate at the petiole. To predict LMA, the following equation was used:

$$predicted\ LMA = (Petiole\ Width)^2/(Leaf\ Area) \quad (3)$$

With petiole width in m, and leaf area in m^2 (Royer *et al.,* 2007). In addition to the 32 samples collected in July, an additional 131 leaf sample measurements of UC and US provided by Dr. Alex Cheesman were used. The leaf samples were not averaged by branch for this analysis, rather the single petiole width and same leaf area was used for the equation. Predicted LMA was then plotted against measured LMA and linear regression performed to test whether a relationship existed.

A linear regression was performed on leaf traits which were predicting LMA. A linear regression was also applied to Cell Area as a predictor of UI. As Cell area and LMA had a non-linear response, a $\log_{10}$ transformation of LMA and cell area was applied to the data to obtain a linear equation.

3.9 Statistical Analysis

A least-squares regression was used in GraphPad to correlate leaf traits and LAI to obtain relevant statistical values (regression equation, r^2 and P-values). Each trait ($\delta^{13}C$, LMA, Cell area and UI value) was presented as a straight within species comparison between the US and UC. To display variance between the traits taken from the drought UC and control UC, an unpaired t-test was performed for each leaf trait. The parametric test assumed a gaussian distribution. A significance level of $P<0.05$ was considered for this comparison. The same data analysis was performed on differences between the gap and understory samples. A linear regression was performed for each trait by species against LMA.

Measurements from all three data sets were used to scale LMA against petiole width, to test the method of reconstruction calculated by Royer *et al.,* (2007). Traits were then

compared against one another with a least-squares regression to identify potential correlations.

A linear regression was performed on leaf traits which were predicting LMA. A linear regression was also applied to Cell Area as a predictor of UI. As Cell area and LMA had a non-linear response, a $\log_{10}$ transformation of LMA and cell area was applied to the data to obtain a linear equation.

APPENDIX B: NON-SIGNIFICANT INTER-CORRELATED TRAITS

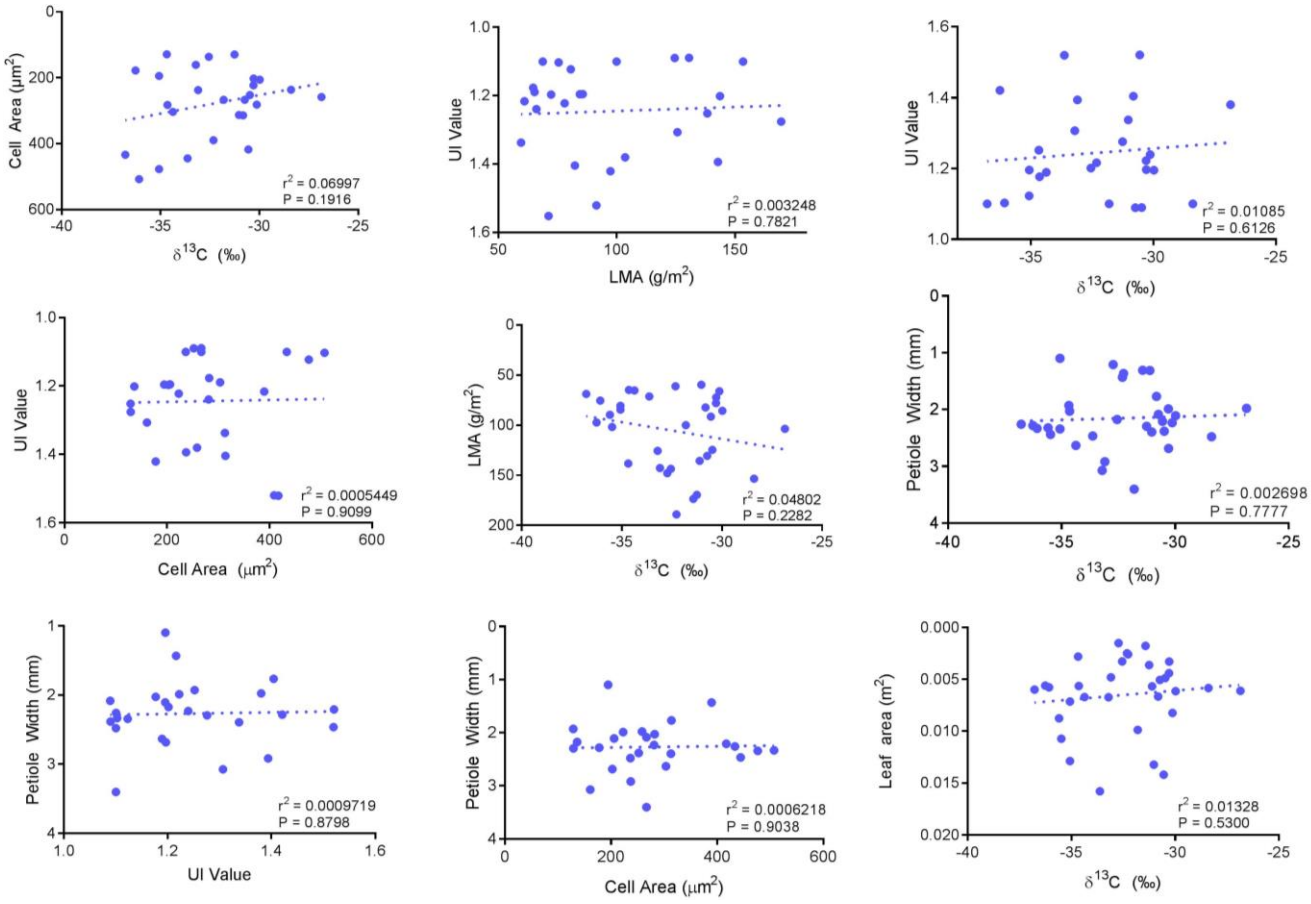

Appendix B: Non-significant results of species comparisons.

APPENDIX C: DATA PRESENTED AND STATISTICAL ANALYSIS OF TRAITS

				$\delta^{13}C$	LMA (g/m^2)		CA (µm^2)		UI		Leaf Area (m^2)		Leaf Mass (m^2)		P Width (m)
HD	Species	Location	LAI	Average	Average	Std. dev.	Average	Std. dev.	Average	Std. dev.	Average	Std. dev.	Average	Std. dev.	Average
	A. peralatum	CC	0.56	-31.11	135.50	76.54	NA	NA	NA	NA	0.0026	0.0012	0.4945	0.2406	0.00137
		IC	1.17	-32.27	189.01	10.24	NA	NA	NA	NA	0.0015	0.0003	0.2218	0.0491	0.00121
		CC-D	0.47	-31.43	173.55	4.37	NA	NA	NA	NA	0.0088	0.0028	0.7220	0.0952	0.00232
		IC-D	0.86	-32.73	147.87	3.11	NA	NA	NA	NA	0.0107	0.0012	1.0910	0.1156	0.00244
		US	6.18	-35.59	89.65	35.09	NA	NA	NA	NA	0.0057	0.0043	0.5522	0.1368	0.00131
		US-GAP	4.94	-35.49	101.83	1.18	NA	NA	NA	NA	0.0018	0.0005	0.3088	0.0881	0.00131
	C. myrianthus	CC	1.69	-29.98	85.62	1.96	205.90	34.64	1.20	0.015	0.0061	0.0016	0.5239	0.1257	0.00211
		IC	4.09	-30.13	66.09	4.44	281.22	14.80	1.24	0.020	0.0082	0.0048	0.5524	0.3481	0.00223
		CC-D	0.95	-30.30	77.99	4.59	222.75	52.99	1.22	0.028	0.0044	0.0016	0.3387	0.1030	0.00199
		IC-D	1.96	-30.29	72.25	3.56	202.40	77.00	1.20	0.018	0.0033	0.0010	0.2358	0.0608	0.00269
		US	5.92	-34.37	65.28	2.06	303.39	58.63	1.20	0.009	0.0067	0.0016	0.4398	0.1183	0.00263
		US-GAP	3.36	-34.64	64.69	4.19	282.13	68.10	1.18	0.026	0.0056	0.0012	0.3621	0.0586	0.00203
	E. microneura	CC-D	0.08	-32.55	143.64	11.12	136.30	18.72	1.20	0.015	0.0028	0.0006	0.3893	0.0905	0.00193
		IC-D	0.62	-34.68	138.33	6.47	128.71	11.43	1.25	0.043	0.0067	0.0031	0.8535	0.4242	0.00307
		CC	0.51	-31.26	169.51	4.63	129.04	23.34	1.28	0.062	0.0056	0.0014	2.0328	0.5200	0.00228
		IC	1.52	-33.21	125.63	5.79	160.75	39.70	1.31	0.018	0.0048	0.0004	0.6997	0.4071	0.00292
		US	7.02	-36.27	97.31	1.71	177.73	19.17	1.42	0.049	0.0033	0.0006	0.4730	0.1181	0.00218
		US-GAP	3.55	-33.10	142.75	74.10	237.15	23.73	1.40	0.082	0.0036	0.0007	0.6124	0.0985	0.00230
	M. globosa	CC	0.16	-28.39	153.39	9.23	236.44	11.60	1.10	0.037	0.0099	0.0020	0.9793	0.1461	0.00340
		IC	2.82	-31.80	99.92	6.73	266.84	27.50	1.10	0.018	0.0049	0.0007	0.6079	0.0953	0.00238
		CC-D	0.88	-30.48	124.52	3.76	252.17	74.38	1.09	0.006	0.0051	0.0025	0.6628	0.3252	0.00209
		IC-D	1.82	-30.74	130.55	5.39	266.96	26.03	1.09	0.004	0.0058	0.0008	0.4374	0.0770	0.00233
		US	7.17	-36.08	75.49	3.63	507.17	99.64	1.10	0.027	0.0071	0.0007	0.5757	0.0696	0.00234
		US	6.69	-35.07	80.57	3.26	476.66	46.48	1.12	0.008	0.0060	0.0019	0.4071	0.1102	0.00226
		US-GAP	5.14	-36.78	68.75	3.85	433.50	47.27	1.10	0.018	0.0058	0.0012	0.8998	0.2259	0.00248
	R. angustifolia	CC	2.51	-30.82	82.31	3.36	313.78	8.10	1.40	0.025	0.0067	0.0009	0.5466	0.0569	0.00177
		IC	3.36	-31.03	59.60	2.46	312.93	25.60	1.34	0.015	0.0132	0.0047	0.7882	0.2761	0.00240
		CC-D	1.82	-26.85	103.53	1.84	258.41	135.20	1.38	0.148	0.0061	0.0028	0.6339	0.2962	0.00198
		IC-D	3.31	-30.56	91.44	7.23	417.19	29.61	1.52	0.092	0.0142	0.0035	1.3138	0.4058	0.00221
		US	6.59	-33.63	71.17	4.60	408.72	168.40	1.52	0.036	0.0158	0.0051	1.1392	0.4231	0.00247
		US-GAP	3.36	-35.07	84.39	10.21	194.39	18.19	1.20	0.210	0.0129	0.0022	1.0754	0.1226	0.00110

AC	Archontophoenix alexandrae	UC	*N/A*	-26.48	123.60	*N/A*	219.97	18.82	1.27	*0.020*	0.0181	N/A	*N/A*	*N/A*	N/A
	Argyrodendron peralatum	UC	*N/A*	-31.84	205.68	*N/A*	*N/A*	*N/A*	*NA*		0.0026	N/A	*N/A*	*N/A*	0.00292
	Brombya platynema	UC	*N/A*	-31.69	106.08	*N/A*	266.11	18.59	1.13	*0.009*	0.0064	N/A	*N/A*	*N/A*	0.00272
	Calamus australis	UC	*N/A*	-27.57	91.84	*N/A*	271.44	12.30	1.80	*0.128*	0.0079	N/A	*N/A*	*N/A*	N/A
	Castanospermum australe	UC	*N/A*	-28.94	105.40	*N/A*	89.70	4.66	1.18	*0.009*	0.0046	N/A	*N/A*	*N/A*	0.00216
	Cleistanthus myrianthus	UC	*N/A*	-31.12	95.89	*N/A*	213.46	32.29	1.15	*0.022*	0.0055	N/A	*N/A*	*N/A*	0.00215
	Cryptocarya grandis	UC	*N/A*	-28.78	113.43	*N/A*	269.56	49.96	1.13	*0.010*	0.0041	N/A	*N/A*	*N/A*	0.00227
	Cryptocarya murrayi	UC	*N/A*	-30.76	125.29	*N/A*	235.50	6.55	1.27	*0.018*	0.0135	N/A	*N/A*	*N/A*	0.00450
	Elaeocarpus angustifolius	UC	*N/A*	-29.16	139.44	*N/A*	148.48	69.41	1.13	*0.032*	0.0022	N/A	*N/A*	*N/A*	0.00173
	Endiandra leptodendron	UC	*N/A*	-30.85	135.04	*N/A*	300.08	29.09	1.15	*0.024*	0.0078	N/A	*N/A*	*N/A*	0.00208
	Endiandra leptodendron	UC	*N/A*	-36.76	65.85	*N/A*	191.02	3.28	1.18	*0.020*	0.0115	N/A	*N/A*	*N/A*	N/A
	Endiandra microneura	UC	*N/A*	-32.81	153.64	*N/A*	137.43	88.44	1.22	*0.010*	0.0027	N/A	*N/A*	*N/A*	0.00220
	Hypserpa decumbens	UC	*N/A*	-29.48	43.63	*N/A*	386.62	138.60	1.17	*0.012*	0.0056	N/A	*N/A*	*N/A*	0.00144
	Myristica globosa subsp. mu	UC	*N/A*	-29.95	126.74	*N/A*	285.87	45.25	1.10	*0.005*	0.0081	N/A	*N/A*	*N/A*	0.00292
	Normanbya normanbyi	UC	*N/A*	-30.44	140.49	*N/A*	532.89	56.11	1.19	*0.019*	0.0153	N/A	*N/A*	*N/A*	0.00703
	Rockinghamia angustifolia	UC	*N/A*	-28.01	104.22	*N/A*	322.80	16.79	1.44	0.058	0.0058	*N/A*	*N/A*	*N/A*	0.00153
LC	Archontophoenix alexandrae	US	*N/A*	-34.08	52.11	0.56	683.88	106.87	1.24	0.031	0.0083	0.0001	0.4304	0.0089	*N/A*
	Argyrodendron peralatum	US	*N/A*	-36.19	92.12	0.57	*N/A*	*N/A*	*N/A*	*N/A*	0.0070	0.0013	0.6478	0.1163	*N/A*
	Brombya platynema	US	*N/A*	-36.48	58.97	7.32	513.42	128.87	1.12	0.006	0.0115	0.0034	0.6600	0.1255	*N/A*
	Calamus australis	US	*N/A*	-36.73	47.47	1.37	466.16	83.36	2.33	0.152	0.0049	0.0001	0.2319	0.0101	*N/A*
	Castanospermum australe	US	*N/A*	-35.88	31.74	1.35	372.02	0.03	1.25	0.040	0.0039	0.0005	0.1252	0.0190	*N/A*
	Cleistanthus myrianthus	US	*N/A*	-34.53	45.32	6.21	348.03	43.95	1.21	0.013	0.0125	0.0007	0.5633	0.0455	*N/A*
	Cryptocarya grandis	US	*N/A*	-34.84	56.24	2.43	552.15	80.30	1.20	0.010	0.0048	0.0012	0.2694	0.0555	*N/A*
	Cryptocarya murrayi	US	*N/A*	-35.99	69.76	2.97	397.62	83.25	1.26	0.066	0.0192	0.0053	1.3327	0.3513	*N/A*
	Elaeocarpus grandis**	US	*N/A*	-36.10	37.40	4.95	436.25	50.54	1.30	0.013	0.0043	0.0002	0.1594	0.0173	*N/A*
	Endiandra microneura	US	*N/A*	-36.92	106.77	8.72	239.28	41.77	1.32	0.010	0.0144	0.0042	1.5412	0.5040	*N/A*
	Hypserpa decumbens	US	*N/A*	-34.66	31.56	16.43	854.66	77.66	1.68	0.062	0.0058	0.0023	0.1616	0.0655	*N/A*
	Myristica globosa subsp. mu	US	*N/A*	-35.37	77.87	7.22	491.63	52.39	1.09	0.007	0.0115	0.0017	0.9003	0.1876	*N/A*
	Normanbya normanbyi	US	*N/A*	-37.29	66.02	48.88	891.34	60.41	1.31	0.086	0.0059	0.0039	0.2830	0.1912	*N/A*
	Rockinghamia angustifolia	US	*N/A*	-32.67	62.61	7.08	573.08	175.04	1.69	0.092	0.0247	0.0073	1.5797	0.6634	*N/A*

Appendix c: Average values of samples and statistical analysis.